2012

New Detection Algorithms for Single Input Multiple Output Systems with Carrier Frequency Offset

Shayondip Sinha
University of Windsor

NEW DETECTION ALGORITHMS FOR SINGLE INPUT MULTIPLE OUTPUT SYSTEMS WITH CARRIER FREQUENCY OFFSET

by

Shayondip Sinha

A Thesis
Submitted to the Faculty of Graduate Studies
through Electrical and Computer Engineering
in Partial Fulfillment of the Requirements for
the Degree of Master of Applied Science at the
University of Windsor

Windsor, Ontario, Canada

2012

New Detection Algorithms For Single Input Multiple Output Systems with Carrier Frequency Offset

by

Shayondip Sinha

APPROVED BY:

Dr. Scott Goodwin
School of Computer Science

Dr. Kemal Tepe
Department of Electrical and Computer Engineering

Dr. Behnam Shahrrava
Department of Electrical and Computer Engineering

TBA
Chair of Defense

18 May, 2012

Co-Authorship Declaration

I hereby declare that this thesis incorporates material that is result of joint research, as follows:

This thesis also incorporates the outcome of a joint research undertaken in collaboration with Garima Deep under the supervision of professor Dr. Behnam Shahrrava. The collaboration is covered in Chapter 4 of the thesis. In all cases, the key ideas, primary contributions, experimental designs, data analysis and interpretation, were performed by the author, and the contributions of co-authors were primarily through the provision of proof reading and reviewing the research papers regarding the technical content.

I am aware of the University of Windsor Senate Policy on Authorship and I certify that I have properly acknowledged the contribution of other researchers to my thesis, and have obtained written permission from each of the co-authors to include the above materials in my thesis.

I certify that, with the above qualification, this thesis, and the research to which it refers, is the product of my own work.

Declaration of Previous Publications

This thesis includes 2 original papers that have been previously submitted for publication in peer reviewed journals and conferences, as follows:

Thesis Chapter	Publication title/full citation	Publication status
Chapter 4	S. Sinha, B. Shahrrava, G. Deep "A New SIMO Detector with Unknown Channel and Carrier Frequency Offset"; IEEE International Global Telecommunication Conference	submitted
Chapter 4	S. Sinha, B. Shahrrava, G. Deep "A New ML Detector for SIMO systems with Imperfect Channel and Carrier Frequency Offset Estimation"; 2012 IEEE Workshop on Signal Processing Systems	submitted

I certify that I have obtained a written permission from the copyright owner(s) to include the above published material(s) in my thesis. I certify that the above material describes work completed during my registration as graduate student at the University of Windsor.

I declare that, to the best of my knowledge, my thesis does not infringe upon anyones copyright nor violate any proprietary rights and that any ideas, techniques,

quotations, or any other material from the work of other people included in my thesis, published or otherwise, are fully acknowledged in accordance with the standard referencing practices. Furthermore, to the extent that I have included copyrighted material that surpasses the bounds of fair dealing within the meaning of the Canada Copyright Act, I certify that I have obtained a written permission from the copyright owner(s) to include such material(s) in my thesis.

I declare that this is a true copy of my thesis, including any final revisions, as approved by my thesis committee and the Graduate Studies office, and that this thesis has not been submitted for a higher degree to any other University or Institution.

Abstract

The performance of a multiple antenna wireless communication (WC) system depends significantly on the type of detection algorithm used at the receiver. This thesis proposes three different types of detection algorithms for single input multiple output (SIMO) systems and concludes with a comparative study of their performance in terms of bit error rate (BER). The proposed algorithms are based on the following classical methods:

- Maximum Likelihood (ML) detection
- Maximal Ratio Combining (MRC) scheme
- Minimum Mean Square Error (MMSE) criterion detection

The major challenge in any practical WC system is the imperfect knowledge of channel state information (CSI) and carrier frequency offset (CFO) at the receiver. The novel algorithms proposed in this thesis aim for optimal detection of the transmitted signal and are derived for a system in the presence of both CSI and CFO estimation errors. They can be treated as a generalized form of their respective type and it is mathematically shown that the conventional algorithms are a special case in the absence of the estimation error. Finally, the performance of the novel algorithms is demonstrated by exhaustive simulation for multi-level modulation techniques of phase shift keying (PSK) and quadrature amplitude modulation (QAM) with increasing values of estimation error variance.

to my

mother, father

and grandmother

Acknowledgements

Hard work paves the way to success, but it is also very important to be shown the right path. I would like to take this opportunity to express by thanks and gratitude to all, who gave me direction and supported me during my time at the University.

Firstly, I would like to thank my supervisor, Dr. Behnam Shahrrava, for his guidance, support and encouragement. He has been a great mentor and his enthusiastic involvement in my research was truly motivational. His valuable suggestions have always helped me academically and also to develop professionally. I would also like to thank Dr. Scott Goodwin and Dr. Kemal Tepe for their invaluable advice. I am thankful to Ms. Andria Ballo, Ms. Shelby Marchand and Mr. Frank Cicchello for providing me with an excellent work environment in the department.

I am highly grateful to all my friends, in particular Dibyendu Mukherjee, Ashirbani Saha, Dr. Gaurav Bhatnagar and Garima Deep for their endless assistance, support and encouragement in the completion of this research.

I dedicate this work to my family and thank them for their love and belief in my abilities.

Table of Contents

List of Figures

List of Acronyms

ASK	Amplitude shift keying
AWGN	Additive white Gaussian noise
BER	Bit error rate
CAFO	Carrier angular frequency offset
CFO	Carrier frequency offset
CSI	Channel state information
ICI	Inter carrier interference
iid	Independent identically distributed
LTE	Long term evolution
MAP	Maximum a posteriori
MIMO	Multiple input antenna and multiple output antenna
MISO	Multiple input antenna and single output antenna
ML	Maximum likelihood
MMSE	Minimum mean square error criterion
MRC	Maximal ratio combining

MSE	Mean square error
OFDM	Orthogonal frequency division multiplexing
PDF	Probability density function
PSK	Phase shift keying
QAM	Quadrature amplitude modulation
QoS	Quality of service
RF	Radio frequency
RV	Random variable
SIMO	Single input antenna and multiple output antenna
SISO	Single input antenna and single output antenna
SNR	Signal to noise ratio
WC	Wireless communication

Glossary of Symbols

$[.]^T$	Transpose of a vector or matrix
$[.]^*$	Complex conjugate of a vector or matrix
$[.]^H$	Hermitian of a vector or matrix
$\|.\|$	Euclidean norm
$\Re\{.\}$	Real value of a variable
$\perp$	Orthogonal
ln	Natural logarithm
$E[.]$	Expected value of a random variable
$Var[.]$	Variance of a random variable
$P(x)$	Probability of the occurrence of x
j	$\sqrt{-1}$
$f(.)$	Probability density function
$A \sim \mathcal{N}(\mu, \sigma_A^2)$	A is a Gaussian random variable with mean μ and variance σ_A^2

Chapter 1

Introduction

The communication industry is undoubtedly the fastest growing sector of the global industrial development as it has made its impact on every stratum of the society. Wireless networks have been a significant contributor since its development from the pre-Industrial age. Signals in the form of torch beams, smokes etc. were predominantly used as wireless signals which eventually lead to the invention of telegraph networks in 1838 by Samuel Morse. This later developed into voice communication, which is prevalent as telephony. Years later in 1895, Marconi performed radio transmission over about 18 miles giving birth to a new genre of WC. Since then, WC has been a hot topic for research and development all across the world. The challenges faced by any communication network is broadly categorized by Weaver [1] as three level problem:

Level A: *Technical problem.*

How accurately the symbols of communication be transmitted?

Level B: *Semantic problem.*

How precisely do the transmitted symbol convey the desired meaning?

Level C: *Effectiveness problem.*

How effectively does the received meaning affect conduct in the desired way?

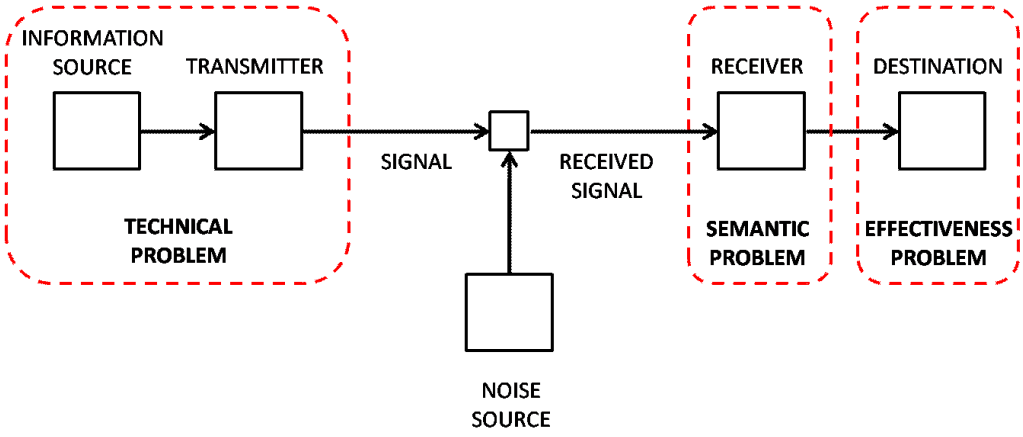

Figure 1.1: Block diagram of a communication system.

Shannon [2] has described these problems with a very basic block diagram of a communication system model as given in Fig. 1.1. The *technical problems* broadly deal with, how accurately the given information is transmitted. This problem is handled by the information source and transmitter blocks. The information source block picks a desired message from a set of possible messages and the transmitter block converts them into signals which are transmitted over the channel. This process employs different encoding methodologies, modulation techniques, diversity schemes, etc. Few of these are broadly discussed in later sections of the thesis. The *semantic problems* are concerned with, how well the receiver interprets the meaning of the information. The transmitted signal undergoes certain level of distortion, or is added with extraneous undesired signals called Noise, while in the communication channel. This deteriorates the quality of the transmission and increases the uncertainty of the receiver to select the original signal. The receiver here acts as an inverse transmitter which converts the signal back to the message at the destination. Lastly, the *effectiveness problems* deal with, how effectively the information or the message is understood by the destination and affects its conduct.

The thesis predominantly concentrates on the *semantic problems* of WC networks. The advent of voice telephony, transmission of high quality video and images require wireless networks to maintain high quality of service (QoS). However, the QoS highly depreciates due to multi path transmission, fading channels etc. In order to obtain a higher QoS in such cases, it is important to achieve reliable data transmission and optimal detection of the data at the receiver. Improvement of 1-dB in signal to noise ratio (SNR) may reduce BER by 90% for an additive white Gaussian noise (AWGN) channel. However, for multi path fading channels similar reduction in BER can be achieved by over 10-dB improvement in SNR.

1.1 MIMO Systems

The performance of a WC system in a multi path fading channel can be significantly improved by employing *diversity* technique where multiple copies of the same information signal is transmitted to the receiver. There are typically five different *diversity* techniques that are used practically [3, 4]:

1. ***Frequency diversity*** - Multiple carriers are used to transmit the same signal.
2. ***Time diversity*** - The same signal is periodically transmitted multiple times.
3. ***Space diversity*** - Multiple antennas are used to transmit or receive multiple copies of the same signal. This technique is also called *Antennae diversity*.
4. ***Polarization diversity*** - The variation of the electric and magnetic fields of the signal is used to achieve multiple transmission.
5. ***Angle diversity*** - Directional antennas are used to create multiple copies of the signal.

Multiple input multiple output (MIMO), systems are most widely researched and implemented in WC systems using *diversity* techniques. MIMO is one of the most optimal approaches for improving reliability of data transmission which does not require additional spectral resources and instead exploits the spatial diversity provided by multiple transmit and receive antennas. Reliability in data transmission is attained when the same data are sent over multiple paths and multiple copies of the data are received with different antennas. Here, the channel capacity is enhanced as the loss of data due to fading in one channel can be compensated for, by the other receiver.

1.1.1 Types of MIMO Systems

MIMO systems can be broadly categorized into two different types

1.1.1.1 Multi-antenna MIMO

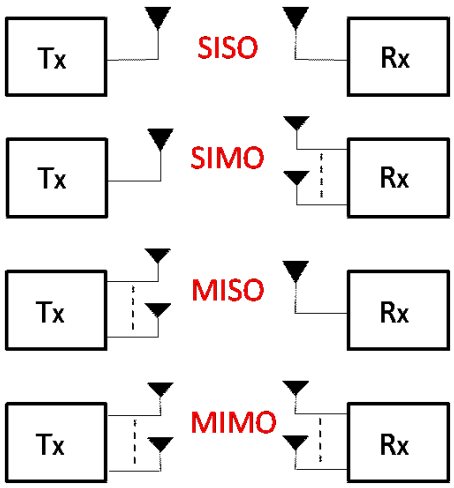

Figure 1.2: Types of multi-antenna MIMO.

A simple block diagram of different multi-antenna MIMO systems are presented in Fig. 1.2.

1. ***Single Input Single Output (SISO)*** - This scheme does not employ any *diversity* technique and is the simplest system with just one antenna at the transmitter and the receiver.

2. ***Single Input Multiple Output (SIMO)*** - Multiple antenna at the receiver is one of the most primitive and widely used MIMO systems [5,6]. This technique is also termed as the *receive diversity* technique, where the multiple copies of the received signal are effectively combined for optimal detection of the transmitted signal. Over a period of time, *diversity* decisions are made at the receiver [7–9] to exploit the robust infrastructure of the base station.

3. ***Multiple Input Single Output (MISO)*** - Multiple antennas at the transmitter, or in other words *transmit diversity* techniques have only been investigated recently [10–13]. Unlike SIMO systems, this technique exploits the *spatial diversity* at the transmitter to create redundancy of the information signal.

4. ***Multiple Input Multiple Output (MIMO)*** - This scheme exploits both *transmit* and receive diversity with multiple antennas for transmission and receiving. MISO systems presented in [11, 12] are also extended for multiple receive antennas.

1.1.1.2 Multi-user MIMO

Multi-user MIMO also known as the MU-MIMO, are advanced MIMO systems which caters to multiple users at the same time in addition to *spatial diversity*.

The work presented in this thesis is performed on SIMO systems as it is the most prevalent and widely implemented MIMO system till date. A survey of different antenna diversity schemes and its evolution is presented in [14, 15]. In practical implementation, multiple antennas are installed at the base station instead of the mobile station for availability of robust infrastructure and capacity. It is also shown

using simulation [11], that multiple antenna scheme at the receiver outperforms the *transmit diversity* schemes. Here, the challenge is to design an algorithm which can process the signal observations from multiple receive antennas to achieve superior performance in terms of BER.

1.2 Modulation and Demodulation

In WC systems, the message signal is modified by the transmitter to make it suitable for transmitting over the channel. This modification is done by altering few parameters of a carrier signal with respect to the message signal and the process is known as *modulation*. As given in [16], *modulation* may be defined as the process by which some characteristic of a signal called *carrier* is varied in accordance with the instantaneous value of another signal called modulating signal. The modulating signal or the message signal is also called the *baseband* signal. Similarly, the recreation of the original message signal from the received signal at the receiver is known as *demodulation*. A survey of different modulation schemes and its effect on WC systems is detailed in [17]. The work presented in this thesis has been simulated for M-ary PSK and QAM modulation types. Fig. 1.3 illustrates their basic block diagram for a complex baseband signal [18].

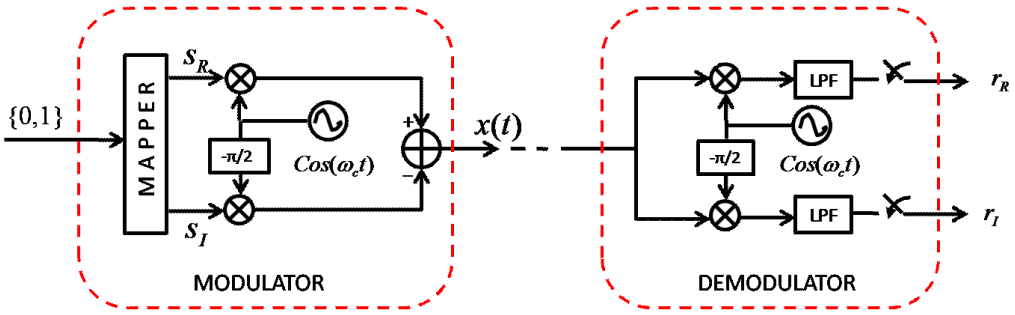

Figure 1.3: Illustration of M-ary PSK/QAM modulation and demodulation

Modulation : The message or the information signal is passed through the mapper where, it maps the message signal depending on the type of modulation. Let us consider, the complex baseband signal from the output of the mapper be $s = s_R + js_I$. The baseband signal is then modulated with a carrier wave of frequency f_c. Thus the radio frequency (RF) signal transmitted from the antenna can be given by

$$\begin{aligned} x(t) &= \Re\left\{se^{(j\omega_c t)}\right\} \\ &= \Re\left\{\left(s_R + js_I\right)\left(\cos\omega_c t + j\sin\omega_c t\right)\right\} \\ &= s_R\cos\omega_c t - s_I\sin\omega_c t, \end{aligned} \tag{1.1}$$

where $\omega_c = 2\pi f_c$.

Demodulation : The RF signal at the receiver is of the form

$$r(t) = r_R\cos\omega_c t - r_I\sin\omega_c t. \tag{1.2}$$

In ideal scenario, the oscillator of the receiver should be tuned at the same carrier frequency f_c. The received signal is then demodulated and at branch one, it becomes

$$\begin{aligned} r(t)\cos\omega_c t &= r_R\cos^2\omega_c t - r_I\sin\omega_c t\cos\omega_c t \\ &= \frac{r_R}{2}\left\{\cos 2\omega_c t + 1\right\} - \frac{r_I}{2}\left\{\sin 2\omega_c t\right\}. \end{aligned} \tag{1.3}$$

It is then passed through a low pass filter and the output is $\frac{r_R}{2}$. Similarly, in branch two

$$\begin{aligned} r(t)\sin\omega_c t &= r_R\cos\omega_c t\sin\omega_c t - r_I\sin^2\omega_c t \\ &= \frac{r_R}{2}\left\{\sin 2\omega_c t\right\} + \frac{r_I}{2}\left\{\cos 2\omega_c t - 1\right\}. \end{aligned} \tag{1.4}$$

This is also passed through a low pass filter with an output $\frac{r_I}{2}$. The signal is further sampled to obtain the digital baseband signal.

1.2.1 Phase Shift Keying

Phase Shift Keying (PSK) is a type of digital modulation scheme that alters or modulates the phase of the carrier signal with reference to the message signal. It is one of the most widely used modulation schemes in MIMO. Fig. 1.4 shows the signal

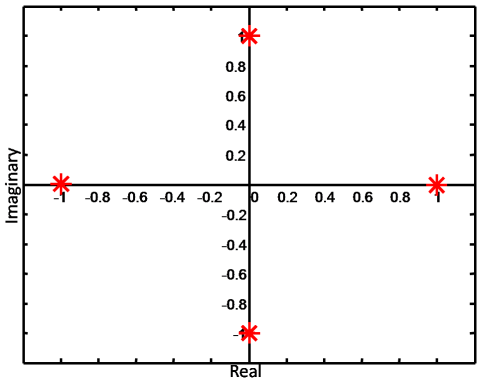

(a) 4-PSK modulation

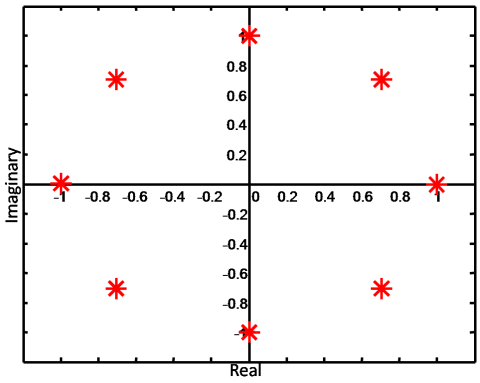

(b) 8-PSK modulation

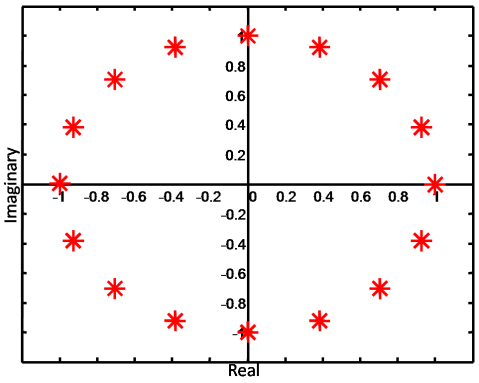

(c) 16-PSK modulation

Figure 1.4: Signal space diagram of PSK modulations.

space diagram of 4-PSK, 8-PSK and 16-PSK modulation schemes. The performance analysis of PSK schemes on different WC systems is studies in [19, 20]. Simulation for the algorithms proposed in this thesis is done on all three PSK schemes states above, to obtain the case for equal energy constellations.

1.2.2 Quadrature Amplitude Modulation

This modulation technique can be used for both analog and digital message signal. For digital signals, the modulated waveform is the combination of PSK and amplitude shift keying (ASK). Fig. 1.5 is the constellation diagram for 4-QAM, 16-QAM and

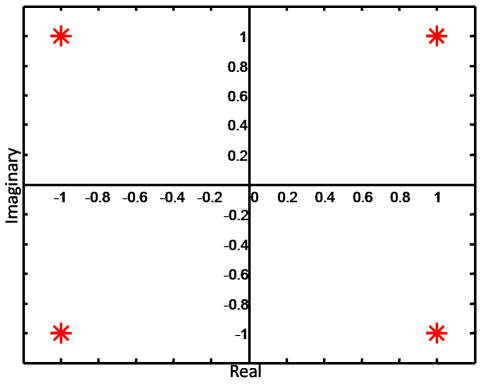

(a) 4-QAM modulation

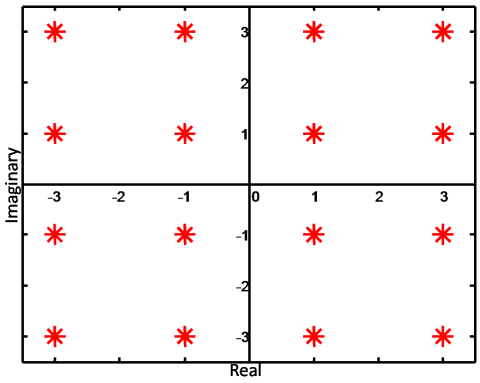

(b) 16-QAM modulation

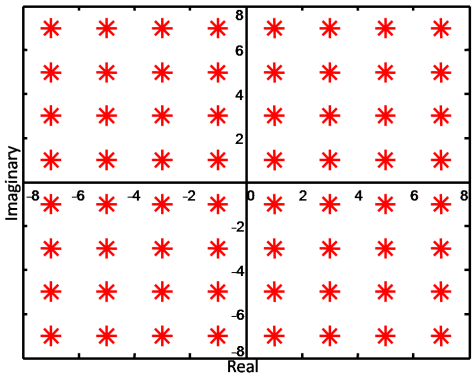

(c) 64-QAM modulation

Figure 1.5: Signal space diagram of QAM modulations.

64-QAM modulations. An analysis of the performance of QAM modulation schemes is done in [21] and the performance of standard detectors with QAM modulation is illustrated in [22]. This modulation scheme is used in the thesis to analyze the performance of the proposed algorithms for symbols with varying energy.

1.3 Motivation and Problem

As stated earlier, one of the major challenges in a WC system is to maintain high QoS. With the advent of new technologies like MIMO as described in section 1.1 and different modulation schemes given in section 1.2, WC systems have become highly susceptible to different parameters that can degrade its QoS drastically. Several factors that affect the performance of wireless systems include AWGN, multi-channel fading and Carrier Frequency Offset (CFO).

1.3.1 Multi-Channel Fading

In a WC system, the propagation of signal does not rely on a specific path. Instead, due to the existence of multiple paths, different copies of the same transmitted signal are received. Multiple paths can be generated, when the electromagnetic signal reflects to a larger surface, diffract from an irregular surface or experience scattering. Fig. 1.6 shows multiple paths taken by a transmitted signal in a typical WC scenario.

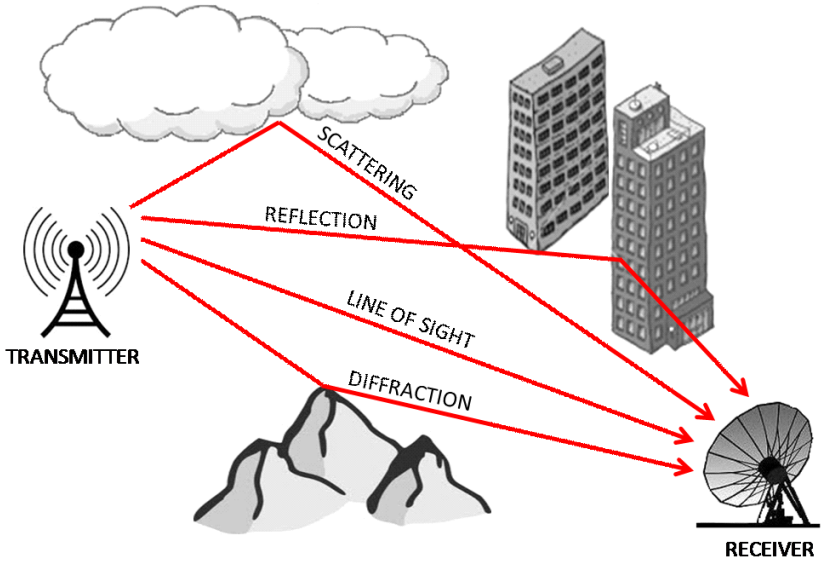

Figure 1.6: Multipath propagation in a wireless channel

The multiple received copies experience different fading due to their respective paths and results in a non additive noise to the system in addition to AWGN. This phenomenon is known as *multipath* or *multi-channel* fading. Multi-channel fading can be categorized [9] as

1. *Flat slow fading* - The signal bandwidth is smaller than the coherence bandwidth of the channel. The signal duration is smaller than the coherence time of the channel.

2. *Flat fast fading* - The signal bandwidth is smaller than the coherence bandwidth of the channel. The signal duration is larger than the coherence time of the channel.

3. *Frequency selective slow fading* - The signal bandwidth is larger than the coherence bandwidth of the channel. The signal duration is smaller than the coherence time of the channel.

4. *Frequency selective fast fading* - The signal bandwidth is larger than the coherence bandwidth of the channel. The signal duration is larger than the coherence time of the channel.

The error performance of different fading channels in studied in [23].

1.3.1.1 Rayleigh fading model

Here, we consider a multipath flat fading channel with M different transmission paths. The total received signal along with AWGN $n(t)$ is

$$\begin{aligned} r(t) &= \sum_{k=1}^{M} A_k \cos\left(\omega_c t + \theta_k\right) + n(t) \\ &= \cos\omega_c t \sum_{k=1}^{M} A_k \cos\theta_k - \sin\omega_c t \sum_{k=1}^{M} A_k \sin\theta_k + n(t), \end{aligned} \tag{1.5}$$

where A_k and θ_k are amplitude and phase of the signal of the k-th path. Due to the uncertainty in the obstacle of the propagation path, the terms $X = \sum_{k=1}^{M} A_k \cos\theta_k$ and $Y = \sum_{k=1}^{M} A_k \sin\theta_k$ are considered random variable (RV). For large number of propagation paths i.e. for large values of M, by central limit theorem [24] parameters X and Y are independent identically distributed (iid) Gaussian RV. Thus the envelope of the received signal $R = \sqrt{X^2 + Y^2}$ follows a Rayleigh distribution with probability distribution function (PDF)

$$f_R(r) = \frac{r}{\sigma^2} e^{\left(\frac{-r^2}{2\sigma^2}\right)}, \qquad r \geq 0, \tag{1.6}$$

where σ^2 is the variance of X and Y. The RF signal in (1.2) can be represented by the form given in (1.5) where $r_R = X$ and $r_I = Y$. It is shown earlier that $r(t) = \Re\{\tilde{r}(t)\}$ where

$$\begin{aligned}
\tilde{r}(t) &= \sum_{k=1}^{M} A_k \left(\cos\left(\omega_c t + \theta_k\right) + j \sin\left(\omega_c t + \theta_k\right)\right) \\
&= \sum_{k=1}^{M} A_k e^{j(\omega_c t + \theta_k)} \\
&= \sum_{k=1}^{M} \underbrace{s\,|\alpha_k|\, e^{j\theta_k}}_{baseband} e^{j\omega_c t}.
\end{aligned}$$

This baseband signal after being sampled with a given sampling time T_s, yields the baseband signal of the form

$$r = \alpha s + n, \tag{1.7}$$

where α is a complex Gaussian RV with its amplitude $|\alpha|$, a Rayleigh RV and s is the transmitted baseband signal. The Rayleigh fading model is the most widely used for simulating a WC channel with diverse modeling methods [25]. The performance of different WC system models and modulation schemes have also been studied [26–29] under the effect of Rayleigh fading over years.

1.3.2 Carrier Frequency Offset

In every WC system, the baseband message signal is transmitted over a carrier signal of a given frequency f_c. This mechanism is known as modulation, which is already discussed in section 1.2. In order to perfectly retrieve the baseband signal, the oscillator at the receiver should be ideally tuned to the frequency of the RF signal. However in practical scenario, the two frequencies differ. This happens due to varied reasons like Doppler shifts and device impairment causing physical differences between the local oscillators of transmitter and receiver. This difference in the frequency is known as CFO and can be expressed in the form

$$\triangle f = f_c - f_r, \tag{1.8}$$

where f_r is the frequency of the receiver oscillator. CFO introduces a frequency shift, and the received signal in (1.5) becomes

$$\begin{aligned} r(t) &= \sum_{k=1}^{M} A_k \cos\left(\left(\omega_c + \triangle\omega_c\right) t + \theta_k\right) + n(t) \\ \therefore \tilde{r}(t) &= \sum_{k=1}^{M} A_k \left(\cos\left(\left(\omega_c + \triangle\omega_c\right) t + \theta_k\right) + j \sin\left(\left(\omega_c + \triangle\omega_c\right) t + \theta_k\right)\right) \\ &= \sum_{k=1}^{M} A_k e^{j((\omega_c + \triangle\omega_c)t + \theta_k)} \\ &= \sum_{k=1}^{M} \underbrace{s\left|\alpha_k\right| e^{j\theta_k} e^{j\triangle\omega_c t}}_{baseband} e^{j\omega_c t}, \end{aligned}$$

which changes the relationship between the transmitted and received baseband signal in (1.7) to the form

$$r = \alpha s e^{j\phi} + n, \tag{1.9}$$

where $\phi = 2\pi\triangle f / f_s$ is the carrier angular frequency offset (CAFO) and f_s is the symbol rate. The representation in (1.9) is valid when $\triangle f_k \ll f_s$, which is typically assumed for any practical wireless system [30].

The advanced standards used in present day WC like long term evolution (LTE) uses multi-carrier modulation schemes like orthogonal frequency division multiplexing (OFDM) which relies greatly on the orthogonality between the sub-carriers. This makes the system highly vulnerable to inter carrier interference (ICI) caused by CFO. Practical systems suffer significant deterioration in performance with both multi-channel fading and CFO as discussed in [31–34]. To mitigate this declension of QoS, CFO has become a hot topic of study among researchers today.

1.4 Objective

The research is targeted to improve the QoS of WC systems affected by different parameters introduced in section 1.3. Ideal detection algorithms are designed with an assumption that the CSI is perfectly known to the receiver and it maintains frequency synchronization with the transmitter. However, practical systems require estimating the channel fading parameters and the CFO. The objective of the work presented in the thesis is to design detection algorithms for a receive diversity system with one transmit and multiple receive antenna in the presence of these estimation errors. The aim is to achieve optimal detection of the transmitted message signal with the erroneous estimates of CSI and CFO available to the receiver. The algorithms are designed for three prevalent detection techniques and their performance is analyzed in terms of BER.

1.5 Organization of Thesis

The rest of the thesis is organized as follows. In Chapter 2, a detailed review of the prevalent detection techniques is introduced with their performance analysis for ideal WC systems. Chapter 3 emphasizes on practical WC systems with CSI and CFO estimation errors along with their effect on the detection techniques. The new

detection algorithms for three different techniques are derived in Chapter 4 and the generalized form for these algorithms are also presented. Chapter 5 explains the simulation method, for the analysis of performance of the proposed algorithms for different modulation schemes. Experimental results are shown for different high values of the estimation error variances. Chapter 6 summarizes the research along with related ideas for future work. All relevant mathematical calculations required for proper understanding of the thesis is presented in Appendix A.

Chapter 2

SIMO Detection Techniques

MIMO, as discussed in chapter 1.1 is the most practically implemented system that can effectively improve the QoS in the presence of multi-channel fading. Among different diversity schemes discussed in chapter 1.1, receive diversity is shown to yield high performance [11] with multiple antennas at the receiver. It is beneficial to practically implement it, as the complex system with multiple antennas is installed at the base station which already has a robust infrastructure. This makes the SIMO system have a wide range of application [35–37] in different wireless systems. The research presented in the thesis is primarily done for a two branch SIMO system with one transmit and two receive antenna. This is further generalized for the cases of multiple receive antennas. Fig. 2.1 demonstrates a simple block representation of the working of a two branch SIMO model. The baseband message signal s is

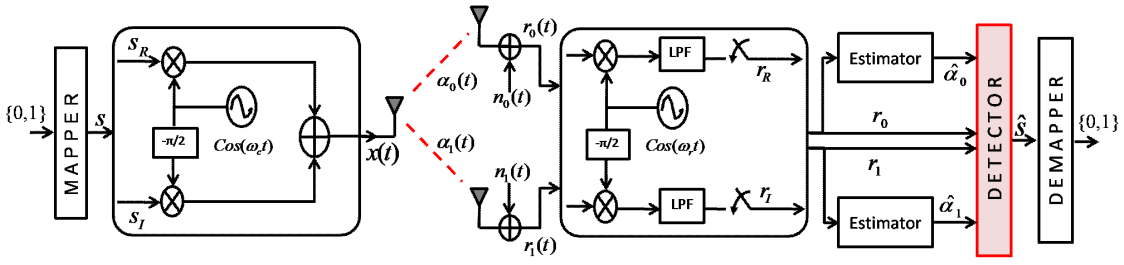

Figure 2.1: Two branch SIMO

modulated and the RF signal $x(t)$ is propagated over the wireless channel using a single transmit antenna. The signal after suffering attenuation due to multi-channel fading and additive noise is received using two antennas. The received signal is further demodulated and sampled to get the baseband signal at the k-th antenna as

$$r_k = \alpha_k s\sqrt{E_s} + n_k, \tag{2.1}$$

where α_k is the channel gain between the transmit antenna and the k-th receive antenna, E_s is the energy per symbol and n_k is the zero mean AWGN with variance σ_n^2 per dimension. This baseband signal is then passed through a detector block for optimal estimation of the transmitted signal. The demapper then converts in into the binary form of the original message or data signal. The main focus of the thesis will be on the detector block at the receiver. The working of different detection schemes for MIMO is explained in [38] and their performance is compared in [39]. The thesis distinctively addresses ML decision detector, linear combiners and MMSE detector for an ideal system ($\hat{\alpha} = \alpha$), which are briefly introduced in section 2.4, section 2.2 and section 2.3 respectively.

2.1 Maximum Likelihood Detection

Maximum Likelihood is a method for detecting unknown parameters based on a set of observations for a given statistic by maximizing the likelihood function. Considering the system model presented in (2.1), the received signal r_k and the channel fading parameters α_k from the k-th receive antenna are taken as the observations, whereas the parameter to be detected is the transmitted signal s. Optimal detection is obtained by choosing from a finite set of symbols $\mathcal{X} = \{\varkappa_0, \varkappa_1, ...\}$ of a given length, depending on the type of modulation scheme. The aim is to obtain the optimum value of $\hat{s} = s$ such that the posterior probability of the transmitted signal conditioned on

the observations is highest. This can be expressed as

$$s \triangleq \arg\max_{s\in\mathcal{X}} \left\{P\left(s|r_k,\alpha_k\right)\right\}. \tag{2.2}$$

The expression is known as *maximum a posteriori* (MAP) probability function. Using Bayes' theorem [24], (2.2) can be written in the form

$$s \triangleq \arg\max_{s\in\mathcal{X}} \left\{\frac{P\left(s\right)P\left(r_k|s,\alpha_k\right)}{\left(r_k\right)}\right\}, \tag{2.3}$$

where the probability of receiving r_k conditioned on α_k and when s is transmitted, $P\left(r_k|s,\alpha_k\right)$ is known as the *likelihood* function. Since we choose the value of $s \in \mathcal{X}$, $P(s)$ is a constant and hence it can be seen from (2.3), that maximizing the likelihood function maximizes the MAP probability. Thus the decision rule for optimal detection becomes

$$s \triangleq \arg\max_{s\in\mathcal{X}} \left\{P\left(r_k|s,\alpha_k\right)\right\}. \tag{2.4}$$

The probability distribution of the received signal r_k can be approximated to be of a Gaussian RV as explained in [40]. The PDF of a Gaussian RV is of the form

$$f(r) = \frac{1}{\sqrt{2\pi\sigma_r^2}} e^{\left(\frac{-\left|r-\mu_r\right|^2}{2\sigma_r^2}\right)}, \tag{2.5}$$

where μ_r is the mean and σ_r^2 is the variance. By taking the negative logarithm of the likelihood function from (2.5), the decision metric in (2.4) becomes

$$\begin{aligned} s &\triangleq \arg\min_{s\in\mathcal{X}} \left\{-\log P\left(r_k|s,\alpha_k\right)\right\} \\ &= \arg\min_{s\in\mathcal{X}} \left\{\left\|r_k-\alpha_k s\right\|^2\right\}. \end{aligned} \tag{2.6}$$

For the case of a two branch SIMO, the ML decision metric for optimal detection of the transmitted signal is

$$s \triangleq \arg\min_{s\in\mathcal{X}} \left\{\left|r_0-\alpha_0 s\right|^2 + \left|r_1-\alpha_1 s\right|^2\right\}. \tag{2.7}$$

ML detection is widely in use for WC systems specially for MIMO. The performance of this detection technique has been studied [41–44] over a period of time, for all

types of MIMO and other wireless systems. This technique has proved to be one of the best in terms of minimizing the BER.

2.2 Linear Combiner

Diversity works, when M independent copies of the transmitted signal is received from the array of M antennas at the receiver. The major challenge in receiver diversity schemes is to effectively detect the data received by these antennas. Diversity combining works by dedicating the signals from the entire array of antennas to form a single signal with the highest SNR. Thus they are more effective when the fading suffered by the multiple copies of the received signal are independent. The most practical approach is linear combiners, for the simplicity of their implementation. Fig. 2.2

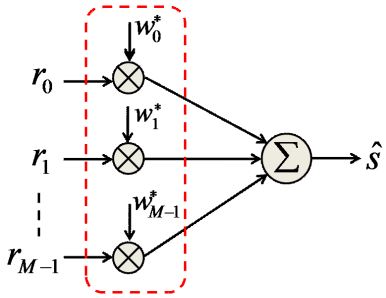

Figure 2.2: Linear Combiner

shows the working of a linear combiner and the generalized form is given as

$$\hat{s} = w_0^* r_0 + w_1^* r_1 + ... + w_{M-1}^* r_{M-1}, \tag{2.8}$$

where w_0, w_1 and w_{M-1} are the weights for optimal combining of the received signal r_0, r_1 and r_{M-1} respectively. Linear combiners are broadly categorized [5, 6] as the following:

1. ***Selection Combining***: This combining scheme opts for the weights of the

signal having the best SNR. The weight selection can be expressed as

$$w = \begin{cases} 1 & \Gamma = \max\limits_{k} \{\Gamma_k\} \\ 0 & \text{otherwise} \end{cases} \tag{2.9}$$

where Γ is the SNR of the signal.

2. ***Equal Gain Combining***: This combining scheme assigns unit gain to all the signals. The general for of linear combiners in (2.8) becomes

$$\hat{s} = r_0 + r_1 + ... + r_{M-1}, \tag{2.10}$$

thus greatly reducing the computational complexity. But it is not an optimal solution in terms of performance.

3. ***Maximal Ratio Combining***: This combining scheme is said to provide optimal solution in terms of SNR [6]. All the signals from the antenna array are combined in a way that the resulting signal has the maximum SNR. The MRC scheme is further discussed in detail.

An elaborate analysis of these combining schemes and their performance is done in [45, 46].

2.2.1 Maximal Ratio Combiner

The general form for a linear combiner given in (2.8) reduced for a two branch SIMO can be given as

$$\hat{s} = W^H R, \tag{2.11}$$

where $W = [w_0 \;\; w_1]^T$ are the combining weights or coefficients and $R = [r_0 \;\; r_1]^T$ are the received signals at two antennas. From (2.1), the above relation can be written as

$$\hat{s} = W^H Z s + W^H N, \tag{2.12}$$

where $Z = [\alpha_0 \quad \alpha_1]^T$ are the channel fading coefficients and $N = [n_0 \quad n_1]^T$ is the AWGN. Here, it is assumed that the receiver has perfect knowledge of CSI. The instantaneous SNR can be expressed as

$$\Gamma = \frac{E\left[\left|W^H Z s\right|^2\right]}{E\left[\left|W^H N\right|^2\right]} = \frac{\sigma_s^2 \left|W^H Z\right|^2}{\sigma_n^2 \left\|W\right\|^2}. \tag{2.13}$$

Here σ_s^2 and σ_n^2 is the variance of the transmitted signal and the additive noise respectively. Cauchy-Schwarz inequality [47] states the following relation

$$\left|\sum_{k=0}^{M-1} w_k \alpha_k\right|^2 \leq \sum_{k=0}^{M-1} \left|w_k\right|^2 \sum_{k=0}^{M-1} \left|\alpha_k\right|^2. \tag{2.14}$$

Thus, maximum SNR can be obtained when $W = Z$. Substituting this relation in (2.13) we get the maximum value of SNR

$$\Gamma_{max} = \frac{\sigma_s^2}{\sigma_n^2} \left\|Z\right\|^2 = \frac{\sigma_s^2}{\sigma_n^2} \left(\left|\alpha_0\right|^2 + \left|\alpha_1\right|^2\right). \tag{2.15}$$

Now, let us substitute the relation $W = Z$ in the general form of linear combiners (2.11), to get the expression for MRC

$$\begin{aligned} \hat{s} &= Z^H R \\ &= \alpha_0^* r_0 + \alpha_1^* r_1, \end{aligned} \tag{2.16}$$

which is optimal in the sense of maximizing SNR.

2.2.2 ML Detector

ML decision is used after MRC for optimal detection of the transmitted signal in terms of BER. For a two branch SIMO system optimal detection can be obtained by choosing the value of s which can minimize the decision metric given in (2.7)

$$\arg\min_s \left\{d^2\left(r_0, \alpha_0 s\right) + d^2\left(r_1, \alpha_1 s\right)\right\}, \tag{2.17}$$

where $d^2\left(x, y\right)$ is the squared euclidean distance between x and y which is calculated as

$$d^2\left(x, y\right) = \left(x - y\right)\left(x^* - y^*\right). \tag{2.18}$$

Expanding (2.10) with little manipulation and substituting in (2.11), it can be easily shown that the ML decision metric for optimal detection is

$$\arg\min_{s} \left\{ \left(\alpha_0^2 + \alpha_1^2 - 1\right) |s|^2 + d^2\left(\hat{s}, s\right) \right\} \tag{2.19}$$

and for equal energy constellations like PSK, the metric is reduced to

$$\arg\min_{s} \left\{ d^2\left(\hat{s}, s\right) \right\}. \tag{2.20}$$

2.3 L-MMSE Detector

Linear MMSE detectors are designed for optimal detection of the transmitted signal by minimizing the mean square error (MSE) between the original value and the estimated value. For a WC system, the MMSE detector aims to minimize the MSE between the transmitted signal s and its MMSE estimate $\hat{s}$. Now, let us consider the case of a two branch SIMO. The system model can be mathematically expressed in the form

$$R = Zs + N, \tag{2.21}$$

where $R = [r_0 \;\; r_1]^T$ are the received signals, $Z = [\alpha_0 \;\; \alpha_1]^T$ are the channel fading coefficients and $N = [n_0 \;\; n_1]^T$ is the AWGN. The general form of a linear estimator is the following

$$\hat{s} = KR \tag{2.22}$$

and the MSE of the detector can be expressed as

$$J = E\left[\|s - \hat{s}\|^2\right] \tag{2.23}$$

Fig. 2.3 shows vector diagram depicting the relation between the original value, estimate and MSE. Here, e is the error given by

$$e = s - \hat{s}. \tag{2.24}$$

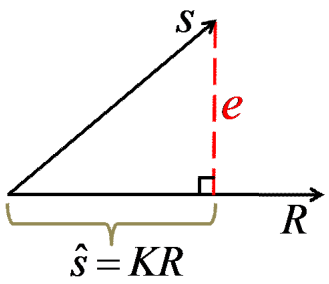

Figure 2.3: Vector diagram of MSE

Orthogonality principle [48] states that an estimator achieves MMSE if and only if the MSE is orthogonal to the observation. i.e. for J_{min},

$$\begin{aligned} & e \perp R \\ \Rightarrow\ & E\left[eR^H\right] = 0 \\ \Rightarrow\ & E\left[(s-\hat{s})\,R^H\right] = 0 \\ \Rightarrow\ & E\left[(s-KR)\,R^H\right] = 0 \\ \Rightarrow\ & K = E\left[sR^H\right]E\left[RR^H\right]^{-1}. \end{aligned} \tag{2.25}$$

Now, let us calculate it individually

$$\begin{aligned} E\left[RR^H\right] &= E\left[\begin{bmatrix} r_0 \\ r_1 \end{bmatrix}\begin{bmatrix} r_0 & r_1 \end{bmatrix}^*\right] \\ &= \begin{bmatrix} \sigma_s^2\left|\alpha_0\right|^2 + \sigma_n^2 & 0 \\ 0 & \sigma_s^2\left|\alpha_1\right|^2 + \sigma_n^2 \end{bmatrix}. \end{aligned} \tag{2.26}$$

Similarly, we calculate

$$\begin{aligned} E\left[sR^H\right] &= E\left[\begin{bmatrix} sr_0^* & sr_1^* \end{bmatrix}\right] \\ &= \sigma_s^2\begin{bmatrix} \alpha_0^* & \alpha_1^* \end{bmatrix}. \end{aligned} \tag{2.27}$$

Substituting the results of (2.26) and (2.27) in (2.25),

$$K = \begin{bmatrix} \underbrace{\dfrac{\sigma_s^2\alpha_0^*}{\sigma_s^2\left|\alpha_0\right|^2 + \sigma_n^2}}_{K_0} & \underbrace{\dfrac{\sigma_s^2\alpha_1^*}{\sigma_s^2\left|\alpha_1\right|^2 + \sigma_n^2}}_{K_1} \end{bmatrix}. \tag{2.28}$$

Thus, from (2.22), we get the mathematical expression of linear MMSE detector for a two branch SIMO as

$$\hat{s} = K_0 r_0 + K_1 r_1, \tag{2.29}$$

where K_0 and K_1 can be obtained from (2.28). The performance of the linear MMSE detector in terms of BER and computational complexity for different MIMO schemes is studied in [49] and for the case of multiple users, in [50].

2.4 Performance Simulation for SIMO

This section presents a performance analysis of a two branch SIMO system. The channel is assumed to be a Rayleigh fading channel and the transmitted symbols are complex with QPSK modulation. It is also assumed that the detection of the transmitted symbols is done with perfect knowledge of CSI at the receiver. There also exits a perfect synchronization between the transmitter and receiver oscillators.

Fig. 2.4 shows the performance simulation of a two branch SIMO (one transmit antenna and two receive antennas) having a classical MRC receiver, with a simple system having no antenna diversity (one transmit antenna and one receive antenna). It can be seen from the simulation result that SIMO system provides almost 6-dB gain over the system with no diversity and the performance improves considerably for high values of SNR.

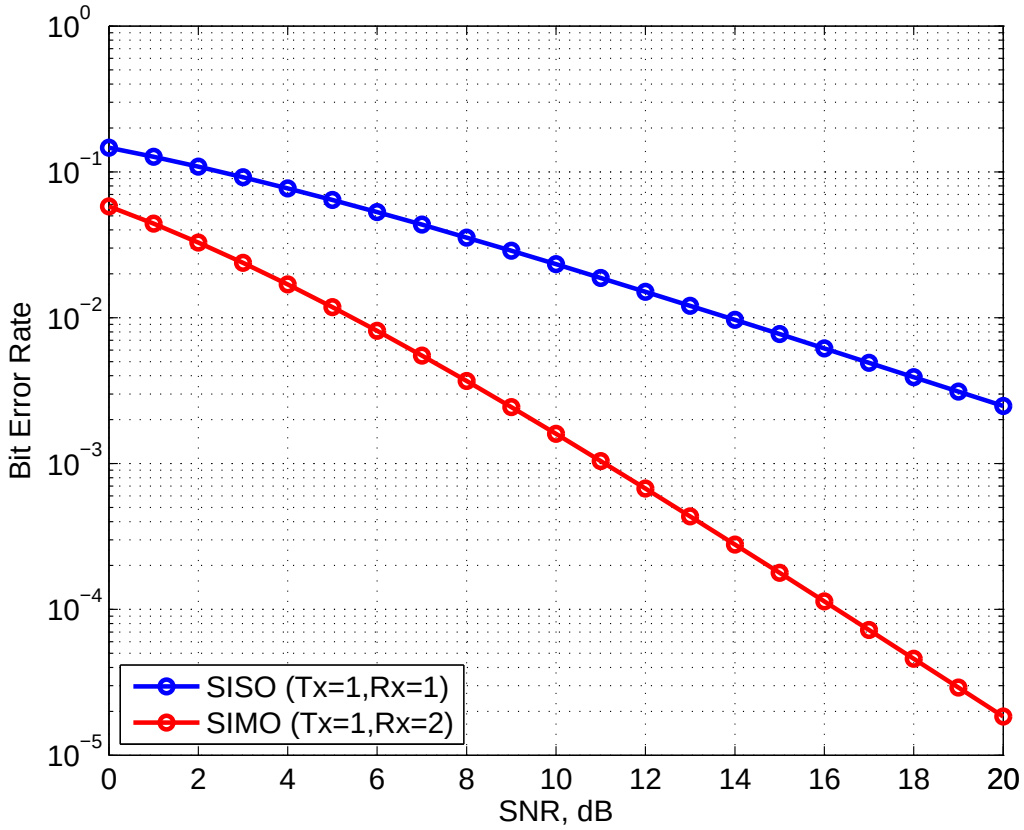

Figure 2.4: Performance of two branch SIMO

Chapter 3

Effect of Imperfect Estimation

This section will focus on the effect of different parameter estimation errors on the detection techniques reviewed in chapter 2. All derivations were done assuming that the receiver is perfectly aware of the CSI and CFO. On the contrary, these parameters are random and require to be estimated at the receiver. This problem has opened doors to a lot of pioneering work to improve upon varying CSI and CFO estimation techniques. However, it is impossible to achieve perfect estimation and thus the detection algorithms are no more optimal. In section 3.1, the effects of channel estimation error is discussed for all the three types of detection techniques and simulation results are shown to compare the performance with an ideal system. Section 3.2 performs a similar analysis with the effect of CFO estimation errors.

3.1 Imperfect Channel Estimation

Let us consider the two branch SIMO model discussed in the previous chapter. The baseband signal at the k-th receive antenna as given in (2.1) is

$$r_k = \alpha_k s\sqrt{E_s} + n_k. \tag{3.1}$$

Here, the channel fading parameters α_k is assumed as a standard normal distribution, i.e. $\alpha_k \sim \mathcal{N}(0,1)$ and the AWGN as $n_k \sim \mathcal{N}(0,\sigma_n^2)$. The output of the channel

estimator is assumed to be erroneous and regardless of the type of estimator used, it can be modeled as

$$\hat{\alpha}_k = \alpha_k + \epsilon_k, \tag{3.2}$$

where $\hat{\alpha}_k$ is the imperfect channel estimate and ϵ_k is the estimation error. Let us consider the case of MMSE channel estimator where we transmit a set of pilot symbols known to the receiver. The baseband signal in (3.1) during the training, can be modified to show the relationship between the received signal and the pilots as

$$r_{k,t} = \alpha_k p_t + n_{k,t}, \tag{3.3}$$

where $P = [p_1 \;\; p_2 \;\; ... \;\; p_l]$ is the set of transmitted pilot symbols of length l and $r_k = [r_{k,1} \;\; r_{k,2} \;\; ... \;\; r_{k,l}]$ is the set of received observation at the k-th antenna. Thus the MMSE estimate of the channel fading parameters can be obtained as

$$\begin{aligned} \hat{\alpha}_k &= \frac{r_k P^H}{PP^H} \\ &= \frac{r_k P^H}{\|P\|^2}. \end{aligned} \tag{3.4}$$

Assuming that the pilot symbols are orthogonal to each other, we can easily write (3.3) as

$$\begin{aligned} & r_k P^H = \alpha_k \|P\|^2 + n_k P^H \\ \Rightarrow \;\; & \alpha_k = \frac{r_k P^H}{\|P\|^2} - \frac{n_k P^H}{\|P\|^2} \\ \Rightarrow \;\; & \hat{\alpha}_k = \alpha_k + \underbrace{\frac{n_k P^H}{\|P\|^2}}_{\epsilon_k}. \end{aligned} \tag{3.5}$$

This relation is similar to the one assumed in [51, 52]. The channel estimation $\epsilon_k \sim \mathcal{N}(0, \sigma_\epsilon^2)$ is considered a zero mean Gaussian RV with variance σ_ϵ^2. Using the relation in (3.2), it can be easily concluded that the imperfect estimate $\hat{\alpha}_k \sim \mathcal{N}(0, \sigma_{\hat{\alpha}}^2)$ is also a Gaussian RV with mean zero and variance $\sigma_{\hat{\alpha}}^2$. The error performance of several MIMO systems under the effect of imperfect channel estimation are studied

in [53–55]. It is proven mathematically, that the estimation error prevents the receiver to achieve optimal detection of the transmitted signal and there by deteriorating the system performance.

3.1.1 ML Detector

ML detector discussed in section 2.4 leads to choosing the optimal value of the transmitted symbol s by maximizing the MAP function

$$s \triangleq \arg\max_{s\in\mathcal{X}} \{P(s|r_k, \alpha_k)\}. \tag{3.6}$$

However in this case, the estimator at the receiver shown in Fig. 3.1 provides imper-

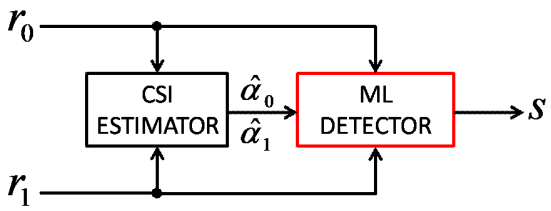

Figure 3.1: ML detector with channel estimator

fect estimate of the channel parameters $\hat{\alpha}_k$ which is given as an input to the detector. This makes the decision metric

$$s \triangleq \arg\max_{s\in\mathcal{X}} \{P(s|r_k, \hat{\alpha}_k)\}. \tag{3.7}$$

By Bayes' theorem introduced earlier, the decision metric leads to maximizing the likelihood function

$$s \triangleq \arg\max_{s\in\mathcal{X}} \{P(r_k|s, \hat{\alpha}_k)\}. \tag{3.8}$$

Taking negative logarithm and using the relation in (3.2), the ML decision metric is given in the form

$$\begin{aligned} s &\triangleq \arg\min_{s\in\mathcal{X}} \left\{ |r_0 - \hat{\alpha}_0 s|^2 + |r_1 - \hat{\alpha}_1 s|^2 \right\} \\ &= \arg\min_{s\in\mathcal{X}} \left\{ |r_0 - (\alpha_0 + \epsilon_0)\, s|^2 + |r_1 - (\alpha_1 + \epsilon_1)\, s|^2 \right\}. \end{aligned} \tag{3.9}$$

This form of ML detection metric involves the channel estimation error ϵ_k and does not provide optimal detection. The degradation of the system performance will be further analyzed by simulation in section 3.1.4.

3.1.2 Linear Combiner

Among all linear combiners, MRC is shown in section 2.2 as the most optimal combiner in the sense of maximizing the SNR of its output. Taking, the general equation of a linear combiner from (2.8), we get

$$\hat{s} = w_0^* r_0 + w_1^* r_1 + ... + w_{M-1}^* r_{M-1}. \tag{3.10}$$

It is shown in section 2.2.1, that the maximum value of combiner output SNR can

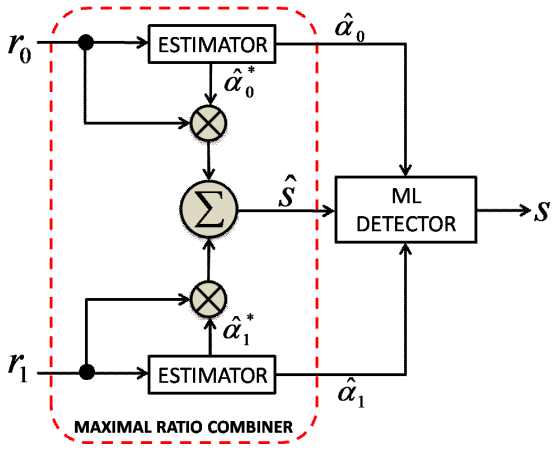

Figure 3.2: MRC with channel estimator

be obtained when $w_k = \alpha_k$. Fig. 3.2 shows that the channel estimates $\hat{\alpha}_k$ known to the receiver is used by the combiner and the MRC scheme becomes

$$\begin{aligned} \hat{s} &= \hat{\alpha}_0^* r_0 + \hat{\alpha}_1^* r_1 \\ &= (\alpha_0 + \epsilon_0)^* r_0 + (\alpha_1 + \epsilon_1)_1^* r_1, \end{aligned} \tag{3.11}$$

which does not provide an output with the maximum SNR and hence is not optimal. Moreover, the ML detector block with the imperfect channel estimates minimizes the decision metric

$$\begin{aligned} s &\triangleq \arg\min_s \left\{ \left(\hat{\alpha}_0^2 + \hat{\alpha}_1^2 - 1 \right) |s|^2 + d^2 \left(\hat{s}, s \right) \right\} \\ &= \arg\min_s \left\{ \left((\alpha_0 + \epsilon_0)^2 + (\alpha_1 + \epsilon_1)^2 - 1 \right) |s|^2 + d^2 \left(\hat{s}, s \right) \right\}. \end{aligned} \tag{3.12}$$

Mathematical model of the BER performance and the SNR of the combiner output is derived in [56–60]. It is shown that the performance of a linear combiner aggravates significantly in the presence of channel estimation error.

3.1.3 L-MMSE

MMSE detector introduced in section 2.3, is one of simplest of all linear estimators and optimal in the sense of minimizing the BER. The MMSE form derived in (2.29)

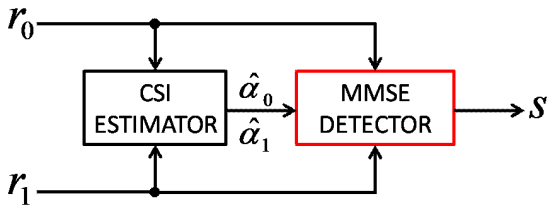

Figure 3.3: MMSE detector with channel estimator

has the coefficient vector K given in (2.28) as

$$K = \left[\frac{\sigma_s^2 \alpha_0^*}{\sigma_s^2 |\alpha_0|^2 + \sigma_n^2} \quad \frac{\sigma_s^2 \alpha_1^*}{\sigma_s^2 |\alpha_1|^2 + \sigma_n^2} \right]. \tag{3.13}$$

If we substitute the channel parameters in (3.13) with the estimates as shown in Fig. 3.3, the coefficient vector becomes

$$\begin{aligned} K &= \left[\begin{array}{cc} \dfrac{\sigma_s^2 \hat{\alpha}_0^*}{\sigma_s^2 \left|\hat{\alpha}_0\right|^2 + \sigma_n^2} & \dfrac{\sigma_s^2 \hat{\alpha}_1^*}{\sigma_s^2 \left|\hat{\alpha}_1\right|^2 + \sigma_n^2} \end{array} \right] \\ &= \left[\begin{array}{cc} \underbrace{\dfrac{\sigma_s^2 (\alpha_0 + \epsilon_0)^*}{\sigma_s^2 \left|(\alpha_0 + \epsilon_0)\right|^2 + \sigma_n^2}}_{K_0} & \underbrace{\dfrac{\sigma_s^2 (\alpha_1 + \epsilon_1)^*}{\sigma_s^2 \left|(\alpha_1 + \epsilon_1)\right|^2 + \sigma_n^2}}_{K_1} \end{array} \right]. \end{aligned} \tag{3.14}$$

It is shown in [61–63] that MMSE detector with the above coefficient does not provide optimal detection.

3.1.4 Performance Simulation

In this section, the performance of a two branch SIMO system is analyzed in the presence of channel estimation error. The channel is assumed to be a Rayleigh fading channel with its parameters having mean zero and unit variance. The channel estimator is taken as a MMSE estimator, as explained earlier in this section and the estimation model $\hat{\alpha}_k = \alpha_k + \epsilon_k$ from (3.5). Let us assume that variance of the AWGN is $\sigma_n^2 = N_0$. Thus as described in [51], by Cramer-Rao bound the minimum value of the estimation error variance is

$$\sigma_\epsilon^2 = \frac{N_0}{l E_s}, \tag{3.15}$$

where l is the length of pilot symbols transmitted during training. The simulation is performed by transmitting 10^4 frames of data symbols with a frame length of 130 symbols. The results are analyzed by plotting the BER against multiple values of SNR. The SNR is defined as σ_s^2/σ_n^2 where σ_s^2 is taken to be unity. The performance is analyzed for multiple values of the estimation error variances by varying the length of the pilot symbols as 4, 8 and 16.

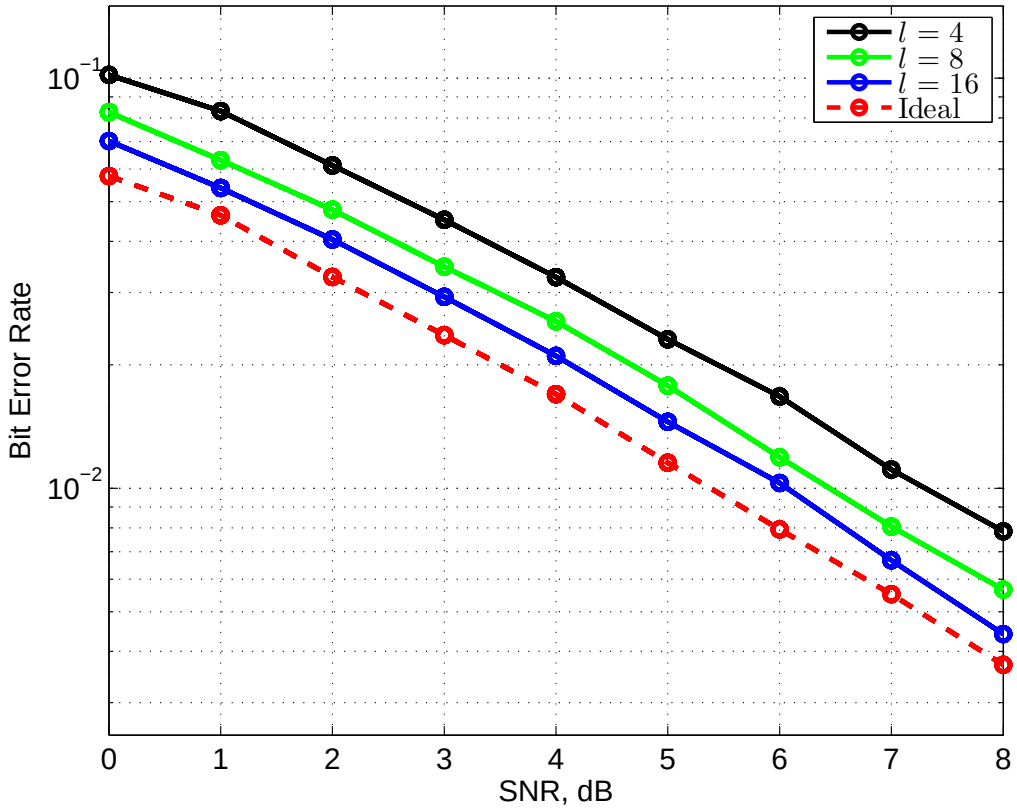

Figure 3.4: Performance of 4-PSK SIMO with channel estimation error

Fig. 3.4 demonstrates the performance of 4-PSK or QPSK modulation scheme in the presence of channel estimation error. It is shown that the performance depreciates for higher values of estimation error and suffers almost 2-dB loss in SNR for a given BER.

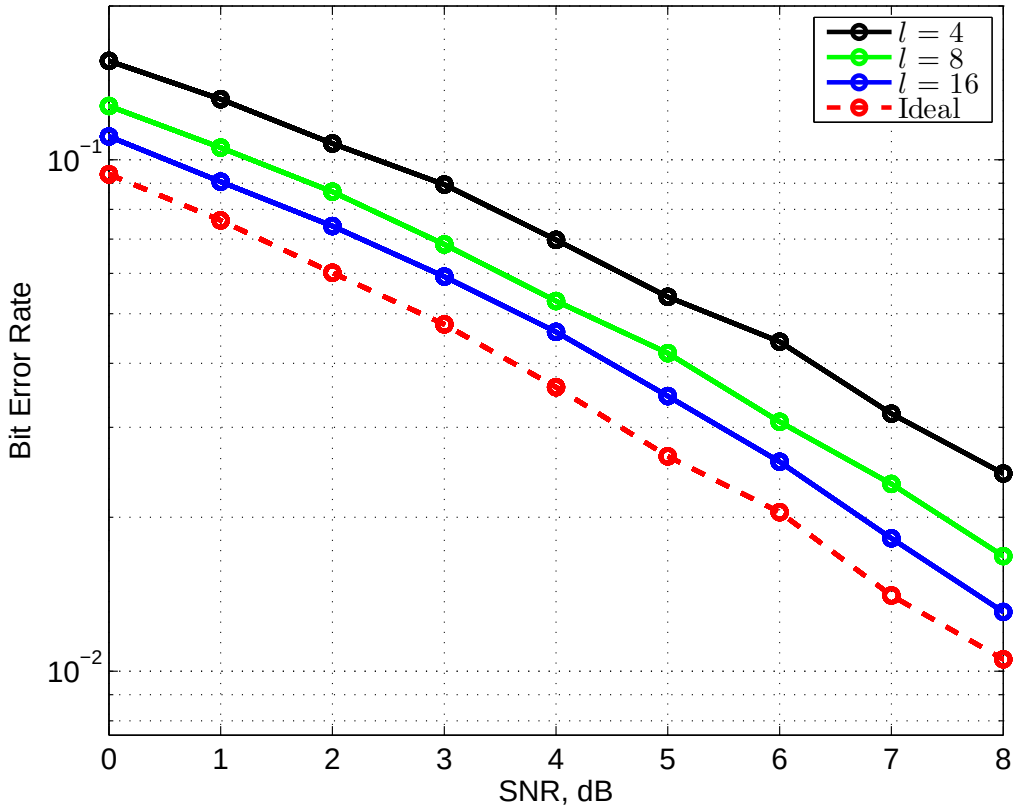

Figure 3.5: Performance of 8-PSK SIMO with channel estimation error

Fig. 3.5 demonstrates the performance of 8-PSK modulation scheme in the presence of channel estimation error. It is shown that the performance suffers almost 2.5-dB loss in SNR for a given BER. It is known from standard literature that the BER performance depreciates for higher modulation schemes. In the presence of estimation error, the depreciation is comparatively high.

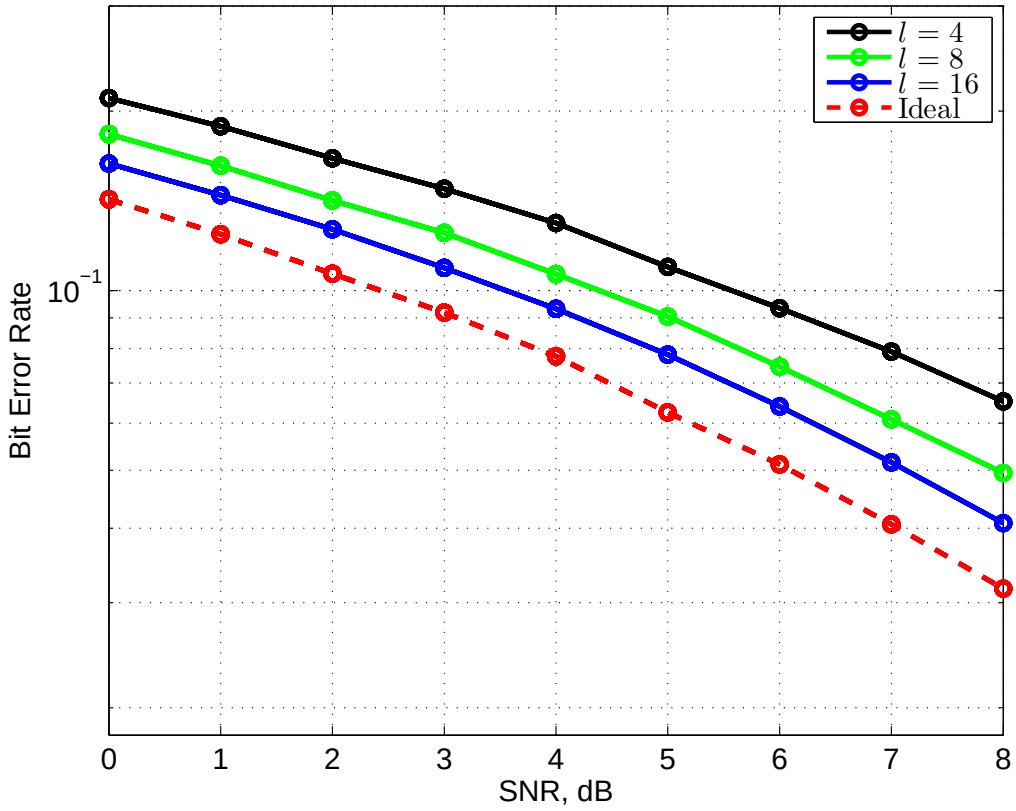

Figure 3.6: Performance of 16-PSK SIMO with channel estimation error

Fig. 3.6 demonstrates the performance of 16-PSK modulation scheme in the presence of channel estimation error. It is shown that the performance suffers almost 3-dB loss in SNR for a given BER. The performance deteriorates from 8-PSK modulation and the deterioration is higher when compared to 4-PSK.

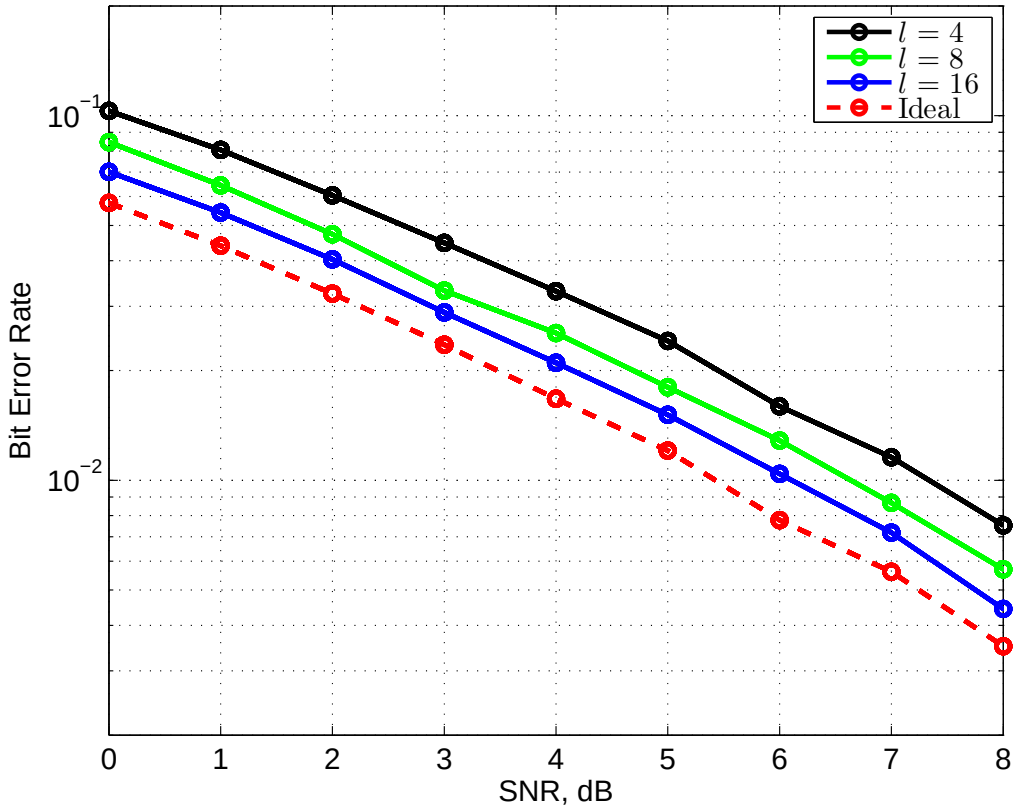

Figure 3.7: Performance of 4-QAM SIMO with channel estimation error

Fig. 3.7 demonstrates the performance of 4-QAM modulation scheme in the presence of channel estimation error. It is shown that the performance suffers almost 2-dB loss in SNR for a given BER and demonstrates identical performance as that of QPSK modulation scheme.

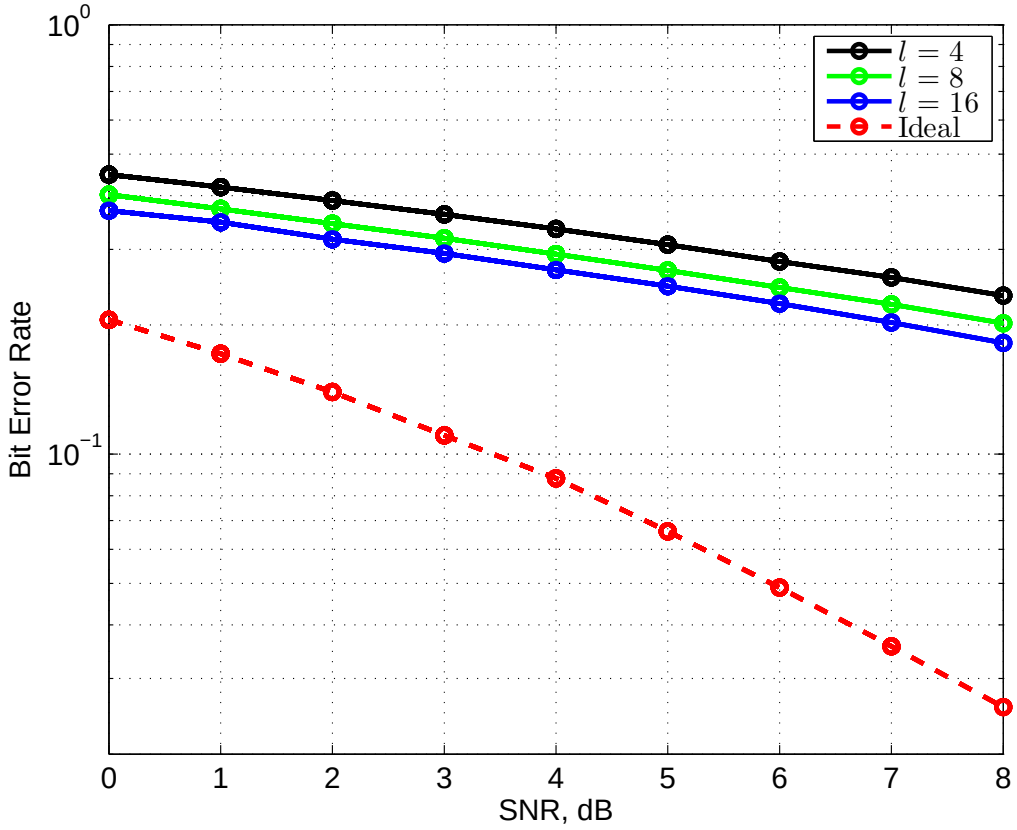

Figure 3.8: Performance of 16-QAM SIMO with channel estimation error

Fig. 3.8 demonstrates the performance of 16-QAM modulation scheme in the presence of channel estimation error. It is shown that the performance suffers almost 7-dB loss in SNR for a given BER. The performance aggravates highly as compared to the 4-QAM modulation as the number of symbols in a constellation increases.

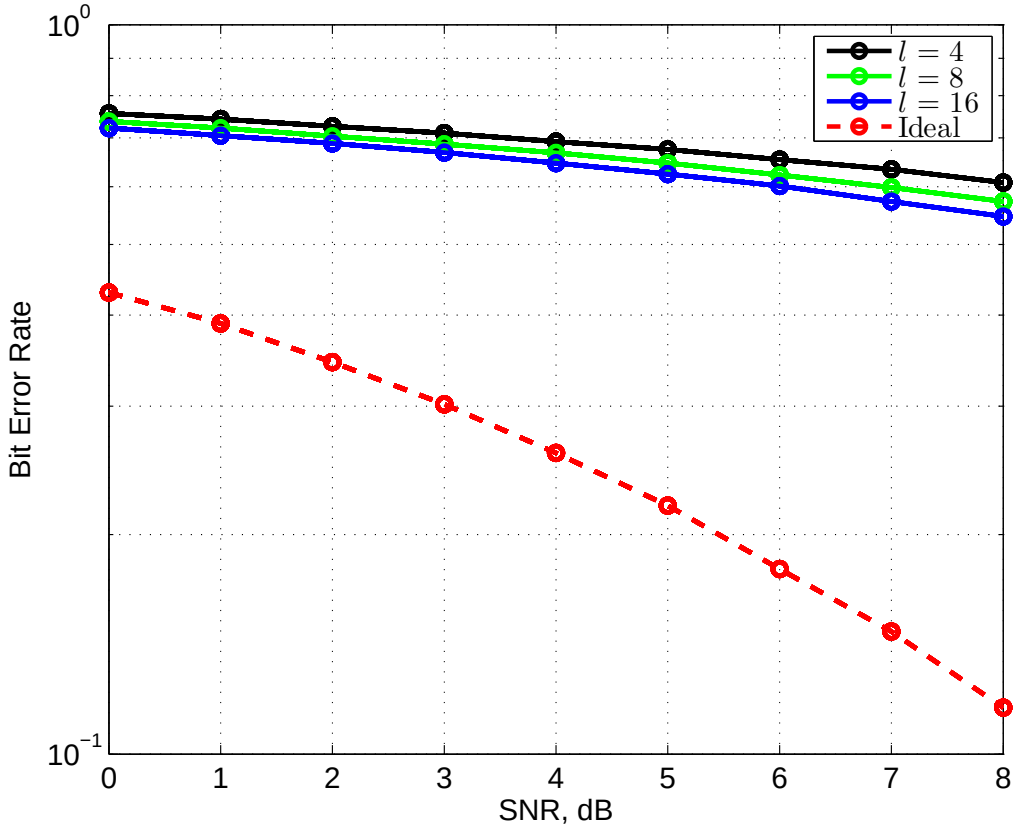

Figure 3.9: Performance of 64-QAM SIMO with channel estimation error

Fig. 3.9 demonstrates the performance of 64-QAM modulation scheme in the presence of channel estimation error. It is shown that the performance suffers over 10-dB loss in SNR for a given BER. This modulation scheme maps 16 symbols to one constellation, thereby making the system vulnerable to high BER.

3.2 Imperfect CFO Estimation

The optimal detection of the transmitted signal can be done, when the RF signal is perfectly demodulated. This requires the frequency of the receiver oscillator to be in perfect synchronization with the carrier frequency of the transmitted RF signal. It is discussed in section 1.3.2, that in practical systems there is a mismatch in the two frequencies. This mismatch is known as CFO and its mathematical relation is given in (1.8). Thus, for a system affected by CFO, the received baseband signal at the k-th antenna is

$$r_k = \alpha_k s e^{j\phi_k}\sqrt{E_s} + n_k, \tag{3.16}$$

where $\phi = 2\pi\triangle f/f_s$ is the CAFO which is assumed to be a Gaussian RV with zero mean and variance σ_ϕ^2, similar to the assumptions made in [64, 65]. The CAFO is unknown to the receiver and is estimated before detection. Irrespective of the type of estimator, the CAFO estimate $\hat{\phi}_k$ is modeled same as that of the channel estimate in (3.2).

$$\hat{\phi}_k = \phi_k + \varepsilon_k \tag{3.17}$$

The estimation error $\varepsilon_k \sim \mathcal{N}(0, \sigma_\varepsilon^2)$ is considered a zero mean Gaussian RV. Since, the original value of CAFO ϕ_k and the estimation error ε_k are independent of each other, the imperfect estimate is also a Gaussian RV $\hat{\phi}_k \sim \mathcal{N}\left(0, \sigma_{\hat{\phi}}^2\right)$. In this section, we consider the most general practical case of a system, in the presence of both CSI and CFO estimation. The system performance highly degrades with effect of these imperfect estimates and its detailed analysis is given in [66–69]. It is also shown using simulation, later in this section.

3.2.1 ML Detector

The ML detector in the presence of channel estimation error maximizes the decision metric given in (3.7). Here we also consider the erroneous estimate of CFO. This

changes the decision metric for choosing $s \in \mathcal{X}$, to

$$s \triangleq \arg\max_{s\in\mathcal{X}} \left\{ P\left(s|r_k, \hat{\alpha}_k, \hat{\phi}_k\right) \right\}. \tag{3.18}$$

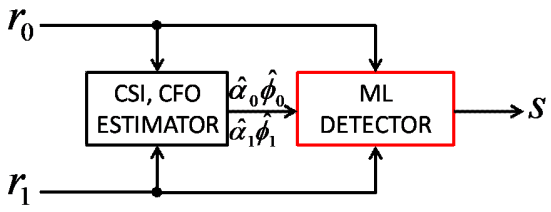

Figure 3.10: ML detector with channel and CFO estimator

Thus by Bayes' theorem, the likelihood function is

$$s \triangleq \arg\max_{s\in\mathcal{X}} \left\{ P\left(r_k|s, \hat{\alpha}_k, \hat{\phi}_k\right) \right\}. \tag{3.19}$$

Using the baseband representation in (3.16), the ML detector in the presence of both channel and CFO estimation error becomes

$$\begin{aligned} s &\triangleq \arg\min_{s\in\mathcal{X}} \left\{ \left| r_0 - \hat{\alpha}_0 s e^{j\hat{\phi}_0} \right|^2 + \left| r_1 - \hat{\alpha}_1 s e^{j\hat{\phi}_1} \right|^2 \right\} \\ &= \arg\min_{s\in\mathcal{X}} \left\{ \left| r_0 - (\alpha_0 + \epsilon_0)\, s e^{j(\phi_0+\varepsilon_0)} \right|^2 + \left| r_1 - (\alpha_1 + \epsilon_1)\, s e^{j(\phi_1+\varepsilon_1)} \right|^2 \right\}. \end{aligned} \tag{3.20}$$

The presence of estimates $\hat{\alpha}_k$ and $\hat{\phi}_k$ of CSI and CAFO respectively does not provide optimal detection. The performance of the ML detector under the mismatch scenario is simulated in section 3.2.4.

3.2.2 Linear Combiner

The combiner relation in (3.11) is derived for imperfect estimates of the channel. However in the presence of CFO estimation, the mathematical expression of the

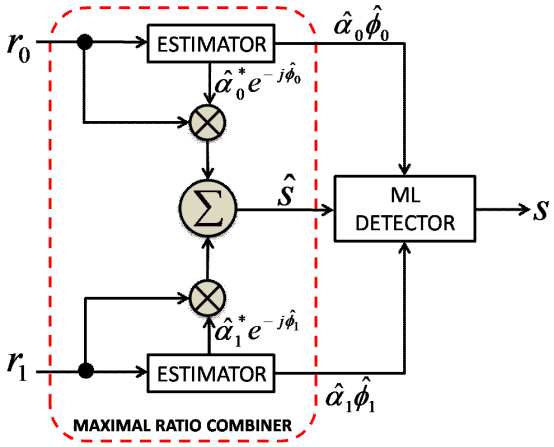

Figure 3.11: MRC with channel and CFO estimator

combiner becomes

$$\begin{aligned}\hat{s} &= \hat{\alpha}_0^* e^{-j\hat{\phi}_0} r_0 + \hat{\alpha}_1^* e^{-j\hat{\phi}_1} r_1 \\ &= (\alpha_0 + \epsilon_0)^* e^{-j(\phi_0+\varepsilon_0)} r_0 + (\alpha_1 + \epsilon_1)_1^* e^{-j(\phi_1+\varepsilon_1)} r_1,\end{aligned} \tag{3.21}$$

which deteriorates the output SNR of the combiner. The effect of CFO estimation error is studied and analyzed for diversity combiners in [66]. However, the ML detector given in (3.12) remains the same and has no effect on its performance by the erroneous CFO estimation.

3.2.3 L-MMSE

The linear MMSE detector derived in (3.14), is in the presence of channel estimation error and it is shown to be no more optimal. As given in Fig. 3.12, in this case the estimator provides the CAFO estimate $\hat{\phi}_k$ along with CSI. Substituting this value,

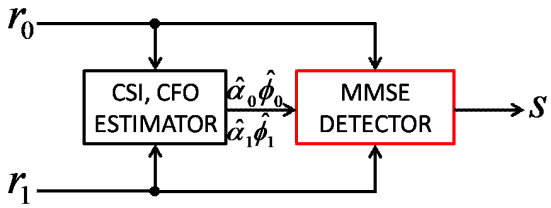

Figure 3.12: MMSE detector with channel and CFO estimator

the MMSE coefficients can be written as

$$K = \left[\begin{array}{cc} \dfrac{\sigma_s^2 \hat{\alpha}_0^* e^{-j\hat{\phi}_0}}{\sigma_s^2 \left|\hat{\alpha}_0\right|^2 + \sigma_n^2} & \dfrac{\sigma_s^2 \hat{\alpha}_1^* e^{-j\hat{\phi}_1}}{\sigma_s^2 \left|\hat{\alpha}_1\right|^2 + \sigma_n^2} \end{array} \right] \tag{3.22}$$

$$= \left[\begin{array}{cc} \underbrace{\dfrac{\sigma_s^2 (\alpha_0 + \epsilon_0)^* e^{-j(\phi_0+\varepsilon_0)}}{\sigma_s^2 \left|(\alpha_0 + \epsilon_0)\right|^2 + \sigma_n^2}}_{K_0} & \underbrace{\dfrac{\sigma_s^2 (\alpha_1 + \epsilon_1)^* e^{-j(\phi_1+\varepsilon_1)}}{\sigma_s^2 \left|(\alpha_1 + \epsilon_1)\right|^2 + \sigma_n^2}}_{K_1} \end{array} \right].$$

The detail analysis of the performance degradation is done in [70].

3.2.4 Performance Simulation

In this section the performance of a two branch SIMO is analyzed in the presence of both CSI and CFO estimation errors. Similar setup is assumed as that of section 3.1.4. The CAFO estimate is modeled as $\hat{\phi}_k = \phi_k + \varepsilon_k$. The variance of CAFO estimation error is considered a simple multiple of the AWGN variance given as

$$\sigma_\varepsilon^2 = a\sigma_n^2 \tag{3.23}$$

where a is any integer. A channel estimator is also assumed with an error variance given in (3.15) with the length of the pilot symbols $l = 16$. Only the CAFO estimation error variance, is altered by the adopting the values $a = 1$, 4 and 9. A comparison is made with a system affected by imperfect channel estimates and not the CFO.

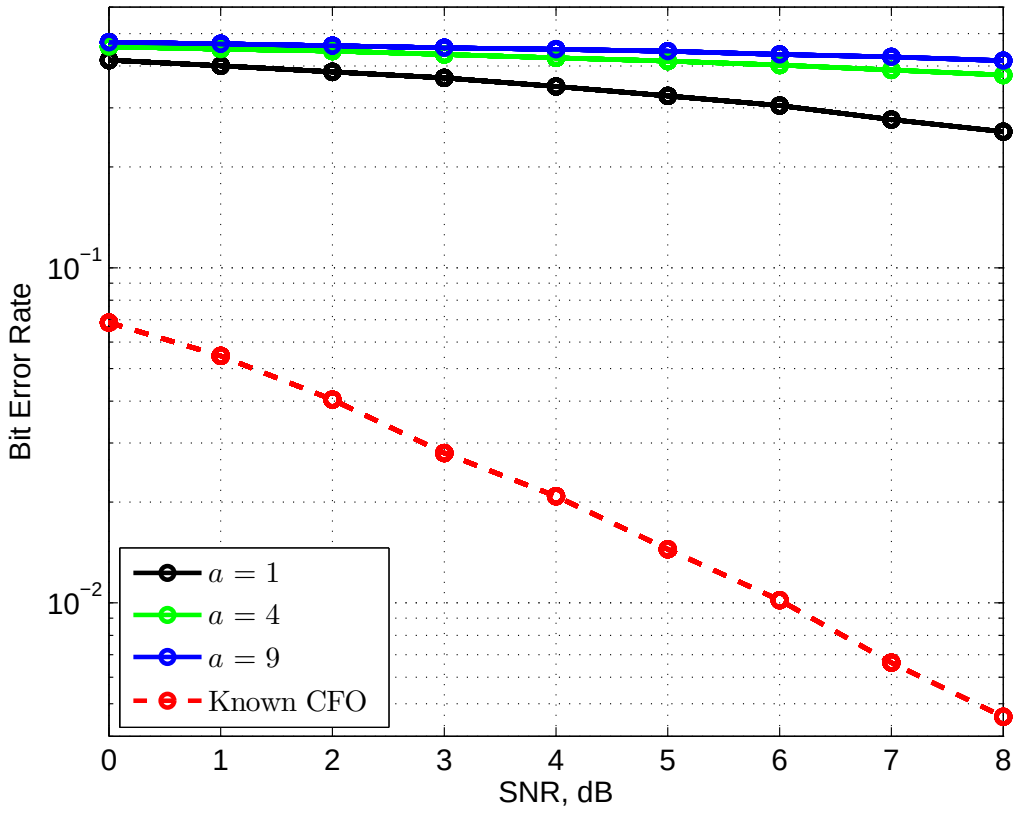

Figure 3.13: Performance of 4-PSK SIMO with CSI and CFO estimation error

Fig. 3.13 demonstrates the performance of 4-PSK or QPSK modulation scheme in the presence of both CSI and CFO estimation error. It is shown that the performance suffers over 10-dB loss in SNR for a given BER.

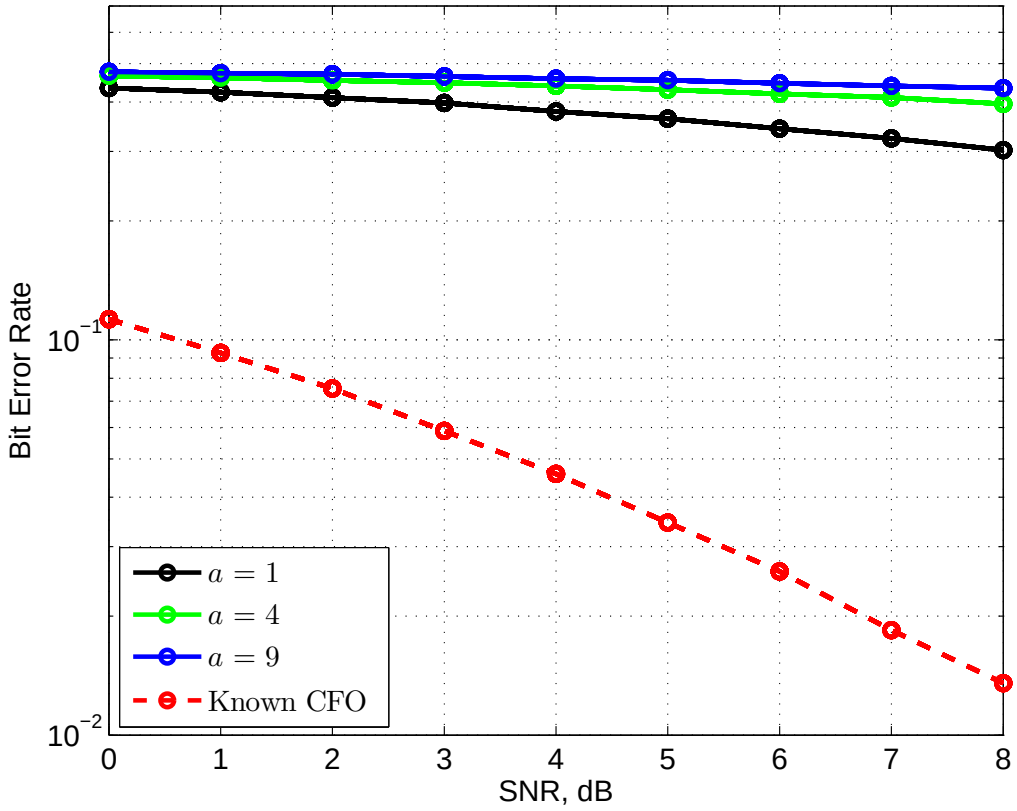

Figure 3.14: Performance of 8-PSK SIMO with CSI and CFO estimation error

Fig. 3.14 demonstrates the performance of 8-PSK in the presence of both CSI and CFO estimation error. It is shown that the performance suffers over 10-dB loss in SNR for a given BER. For higher error variance of the CFO, the performance degrades considerably.

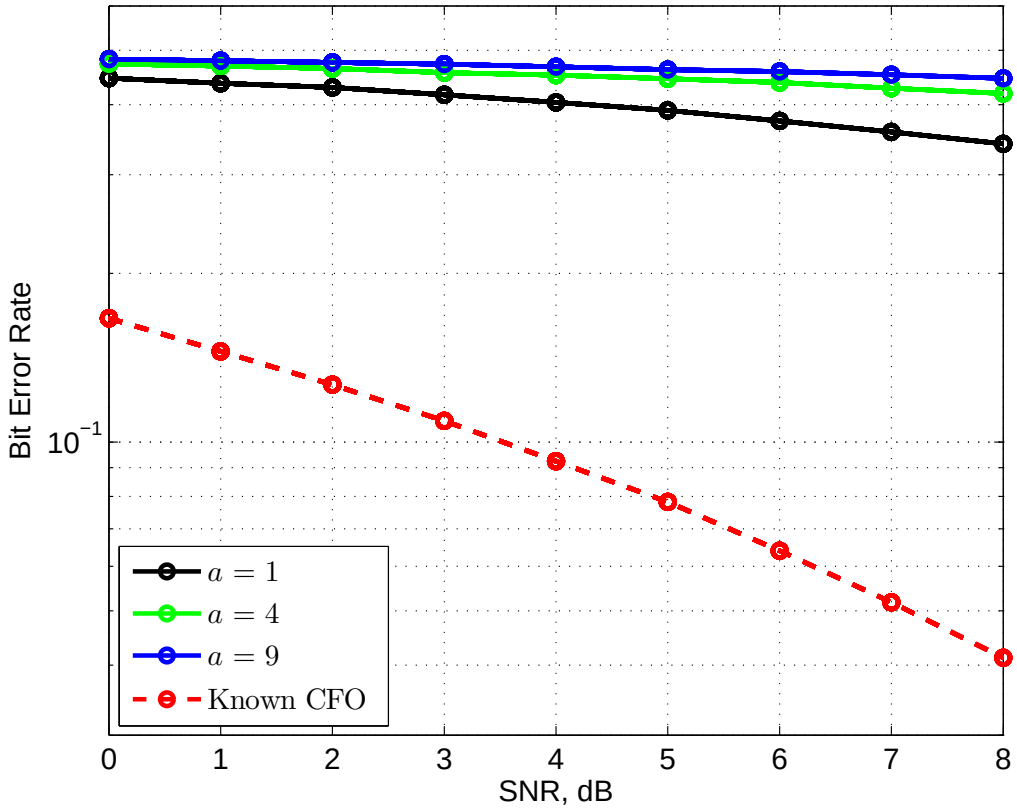

Figure 3.15: Performance of 16-PSK SIMO with CSI and CFO estimation error

Fig. 3.15 demonstrates the performance of 16-PSK in the presence of both CSI and CFO estimation error. It is shown that the performance degrades further than the 8-PSK modulation scheme and suffers a comparatively higher loss than the QPSK scheme.

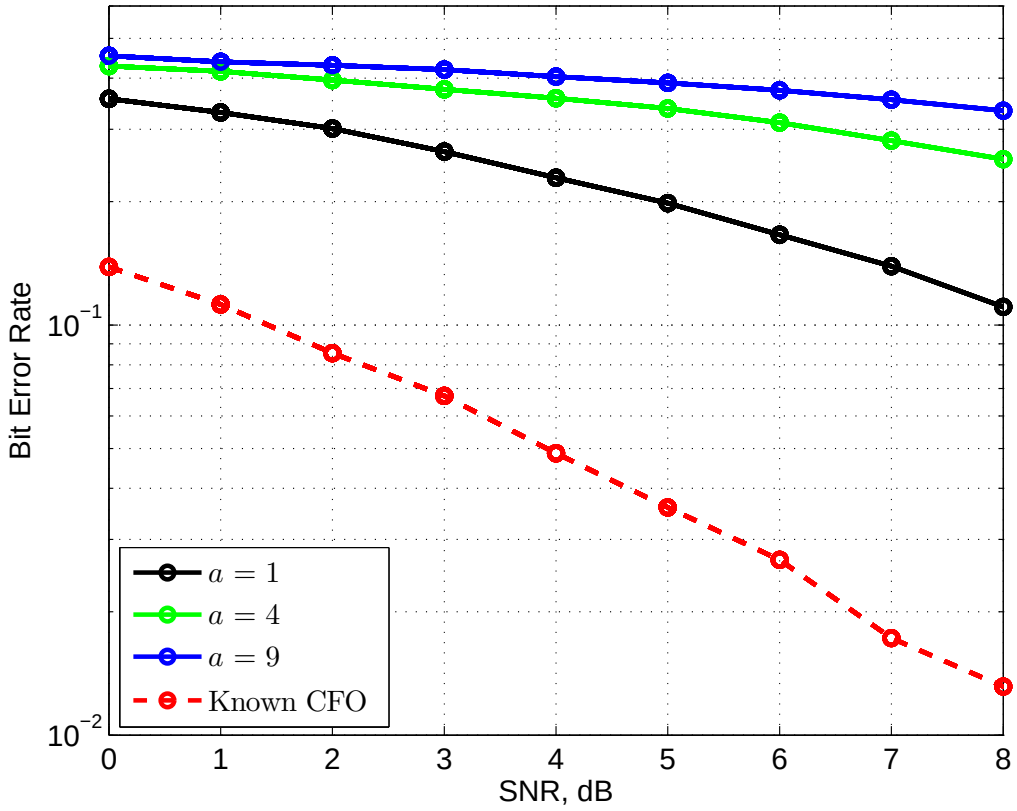

Figure 3.16: Performance of 4-QAM SIMO with CSI and CFO estimation error

Fig. 3.16 demonstrates the performance of 4-QAM in the presence of both CSI and CFO estimation error. The performance demonstrated by this modulation scheme, under the mismatch scenario is identical to QPSK scheme in Fig. 3.13.

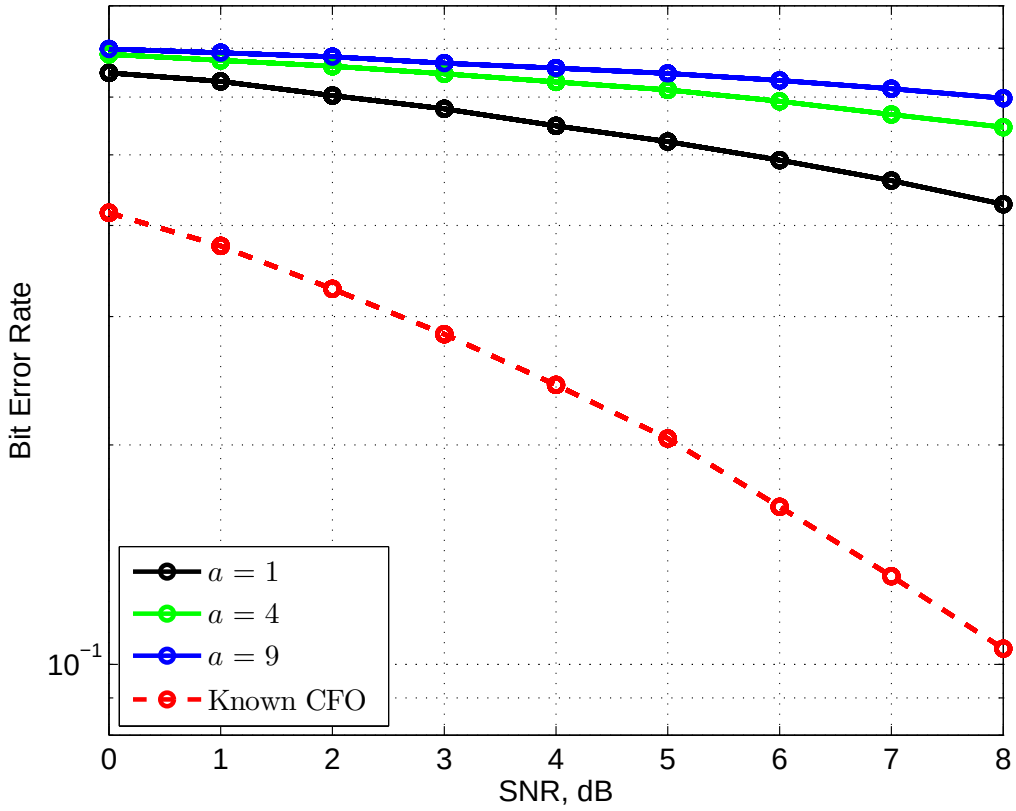

Figure 3.17: Performance of 16-QAM SIMO with CSI and CFO estimation error

Fig. 3.17 demonstrates the performance of 16-QAM in the presence of both CSI and CFO estimation error. This scheme maps 4 symbols per constellation. It is shown by the simulation result that the BER increases with higher modulation.

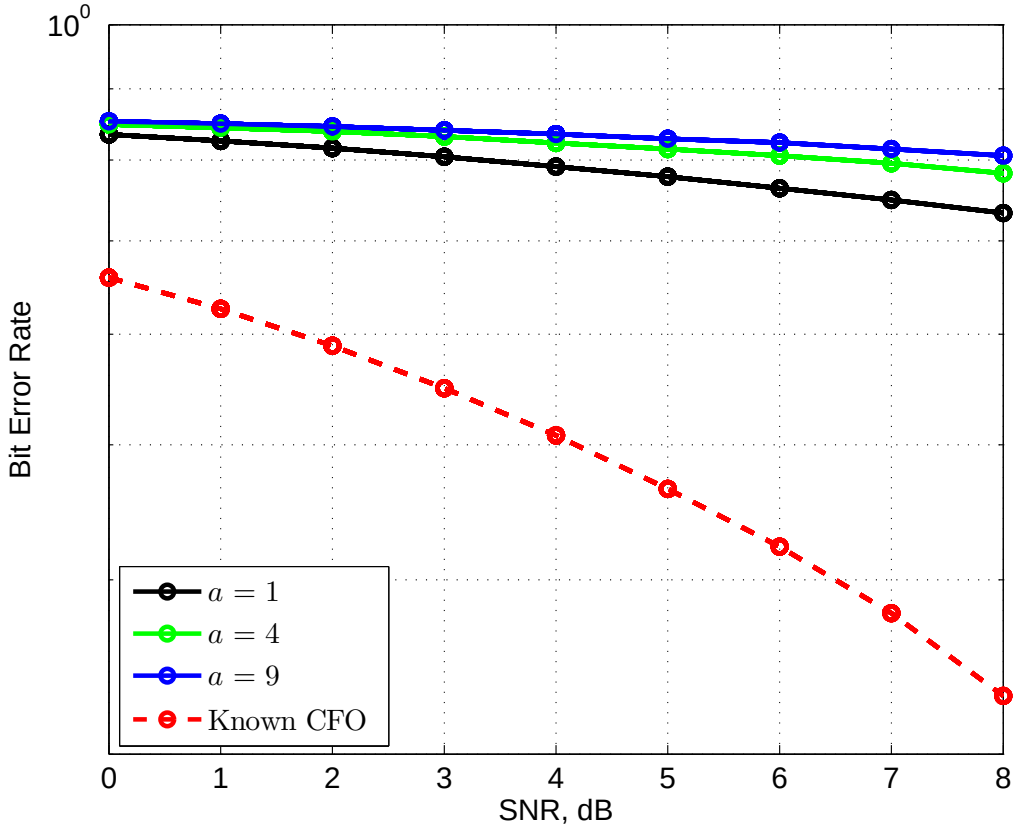

Figure 3.18: Performance of 64-QAM SIMO with CSI and CFO estimation error

Fig. 3.18 demonstrates the performance of 64-QAM in the presence of both CSI and CFO estimation error. This scheme maps 16 symbols per constellation. The performance degrades as compared to the lower modulation schemes.

Chapter 4

Proposed Detection Algorithms in the presence of CSI and CFO estimation errors

This chapter proposes the solution to challenges faced by different WC systems outlined in the previous chapters. Chapter 1, reviews different prevalent diversity schemes. Fading due to multi-channel propagation and the factor of CFO, aggravating the system performance is also introduced. In chapter 2, different detection algorithms along with detail derivations are provided for proper understanding of their performance. These detection algorithms are chosen, because of their extensive use in every practical WC system. The motivation for the research work in this thesis is highlighted in chapter 3. Here, the effect of both channel and CFO estimation errors on SIMO systems is analyzed mathematically for different detection algorithms. Simulations are also performed for different modulation schemes, to demonstrate the system performance under the mismatch scenario. It is shown, that the estimation errors can bring down the system performance significantly. In this chapter, we propose new detection algorithms in the presence of CSI and CFO estimation errors. The new algorithms are based on the detectors discussed earlier in chapter 2 and their detail mathematical derivations are also presented in this chapter.

4.1 Previous Work and Assumptions

As discussed earlier in section 3.1, the channel estimation errors have adverse effect on any WC system. This has opened the door for researchers to design an optimal detector in the presence of channel estimation error. Pioneering work has been done in [51, 71–73] by deriving ML decision metric for optimal detection in the presence of channel estimation errors. However, these decision metrics are derived with an assumption that the receiver frequency is perfectly synchronized with the transmit carrier frequency. The effect of CFO and its estimation error detailed in section 3.2 have also motivated researchers over the period of time. Although, the authors have proposed new detection algorithms for systems affected by CFO in [74–76], the CFO is taken as a deterministic value and is not considered random. In practical systems, where CFO is random and is estimated, these detection algorithms will fail to provide optimal detection of the transmitted signal.

Let us consider a two branch SIMO system presented in Fig. 2.1, with one transmit antenna and two receive antennas. The baseband received signal at the k-th antenna is given in (2.1). The channel parameters, channel estimates and the estimation errors are complex valued Gaussian RVs $\alpha_k \sim \mathcal{N}(0,1)$, $\hat{\alpha}_k \sim \mathcal{N}(0,\sigma^2_{\hat{\alpha}})$ and $\epsilon_k \sim \mathcal{N}(0,\sigma^2_{\epsilon})$ respectively. These three parameters are mathematically related by the form given in (3.2) and the relation between their variances can be easily written as

$$\begin{aligned} \sigma^2_{\hat{\alpha}} &= \sigma^2_{\alpha} + \sigma^2_{\epsilon} \\ &= 1 + \sigma^2_{\epsilon}. \end{aligned} \tag{4.1}$$

It has been already shown in [51, 72], that introducing the correlation between the original channel parameter α_k and the estimate $\hat{\alpha}_k$ into the detection algorithm shows considerable improvement in the system performance. Using the results in [51], the

correlation coefficient can be given as

$$\rho = \frac{1}{\sqrt{1+\sigma_\epsilon^2}}. \tag{4.2}$$

Now, let us consider the system with both CSI and CFO. Here, the baseband signal at the k-th receive antenna is given in (3.16). It is rewritten here for the ease of referring by the mathematical derivations explained ahead in the chapter.

$$r_k = \alpha_k s e^{j\phi_k}\sqrt{E_s} + n_k. \tag{4.3}$$

The CAFO parameters, CAFO estimates and the estimation errors are Gaussian RVs $\phi_k \sim \mathcal{N}\left(0, \sigma_\phi^2\right)$, $\hat{\phi}_k \sim \mathcal{N}\left(0, \sigma_{\hat{\phi}}^2\right)$ and $\varepsilon_k \sim \mathcal{N}\left(0, \sigma_\varepsilon^2\right)$ respectively. From (3.17), the relation between the variances of these parameters can be easily given as

$$\sigma_{\hat{\phi}}^2 = \sigma_\phi^2 + \sigma_\varepsilon^2. \tag{4.4}$$

The correlation coefficient between the original CAFO ϕ_k and the estimate $\hat{\phi}_k$ is calculated as

$$\begin{aligned} \gamma &= \frac{E\left[\phi_k \hat{\phi}_k\right]}{\sqrt{\sigma_\phi^2 \sigma_{\hat{\phi}}^2}} \\ &= \sqrt{1 - \frac{\sigma_\varepsilon^2}{\sigma_{\hat{\phi}}^2}} \end{aligned} \tag{4.5}$$

Using these assumptions, new detection algorithms will be derived in the presence of both CSI and CFO estimation errors. The derivations for the algorithms based of ML detector, linear combiner and MMSE is shown in section 4.2, section 4.3 and section 4.4 respectively.

4.2 ML Detector

This detection method, being one of the most widely used detectors in WC systems; considerable amount of work has already been done. The decision metric proposed by Tarokh et al. [51,71] in the presence of imperfect channel estimates, was primarily derived for space time coded MIMO systems. However, it is now considered as a generalized metric for all MIMO systems. It can be termed as the conventional metric and is still the widely in use for practical systems [77]. Here, the original channel parameter α_k and its estimate $\hat{\alpha}_k$ are taken as bi-variate Gaussian distributed. Thus, the expectation of α_k conditioned on $\hat{\alpha}_k$ is

$$E\left[\alpha_k|\hat{\alpha}_k\right] = \frac{\rho\hat{\alpha}_k}{\sigma_{\hat{\alpha}}} \tag{4.6}$$

and the variance is

$$Var\left[\alpha_k|\hat{\alpha}_k\right] = 1 - |\rho|^2 . \tag{4.7}$$

Using the relation in (2.1), the expectation of the received signal r_k conditioned on $\hat{\alpha}_k$ is calculated as

$$E\left[r_k|\hat{\alpha}_k\right] = \frac{\rho\hat{\alpha}_k\sqrt{E_s}s}{\sigma_{\hat{\alpha}}} \tag{4.8}$$

and the variance as

$$Var\left[r_k|\hat{\alpha}_k\right] = N_0 + \left(1 - |\rho|^2\right) E_s |s|^2 . \tag{4.9}$$

Taking negative logarithm of the likelihood function, the decision metric for a two branch SIMO system was derived as

$$s \triangleq \arg\min_{s\in\mathcal{X}} \sum_{k=0}^{1} \left(\frac{\left| r_k - \frac{\rho\hat{\alpha}_k\sqrt{E_s}s}{\sigma_{\hat{\alpha}}} \right|^2}{N_0 + \left(1 - |\rho|^2\right) E_s |s|^2} + \ln\left(N_0 + \left(1 - |\rho|^2\right) E_s |s|^2\right) \right) \tag{4.10}$$

and for equal energy modulations like PSK, it was reduced to

$$s \triangleq \arg\min_{s\in\mathcal{X}} \sum_{k=0}^{1} \left| r_k - \frac{\rho\hat{\alpha}_k\sqrt{E_s}s}{\sigma_{\hat{\alpha}}} \right|^2 . \tag{4.11}$$

Now, let us consider a system with CFO and the estimate of CAFO available to the receiver is $\hat{\phi}_k$. Taking the estimate into consideration, optimal detection can be obtained maximizing the MAP probability given as

$$s \triangleq \arg\max_{s\in\mathcal{X}} \left\{ P\left(s|r_k, \hat{\alpha}_k, \hat{\phi}_k\right)\right\}. \tag{4.12}$$

This leads to maximizing the likelihood function,

$$s \triangleq \arg\max_{s\in\mathcal{X}} \left\{ P\left(r_k|s, \hat{\alpha}_k, \hat{\phi}_k\right)\right\}. \tag{4.13}$$

With the introduction of CFO, the received signal r_k does not exactly follow a Gaussian distribution. However, it can be shown using simulation, that r_k demonstrates a Gaussian like behavior. Also, by central limit theorem it is appropriate to approximate the received signal as a Gaussian RV, as explained in [40]. Thus, optimal detection of the transmitted signal is obtained by taking negative logarithm of the likelihood function.

$$s \triangleq \arg\max_{s\in\mathcal{X}} \sum_{k=0}^{1} \left(\ln\left(Var\left[r_k|\hat{\alpha}_k, \hat{\phi}_k\right]\right) + \frac{\left|r_k - E\left[r_k|\hat{\alpha}_k, \hat{\phi}_k\right]\right|^2}{2Var\left[r_k|\hat{\alpha}_k, \hat{\phi}_k\right]} \right) \tag{4.14}$$

The values of $E\left[r_k|\hat{\alpha}_k, \hat{\phi}_k\right]$ and $Var\left[r_k|\hat{\alpha}_k, \hat{\phi}_k\right]$ are computed elaborately in Appendix A. For modulations with equal energy like PSK, the decision metric can be modified to

$$\begin{aligned} s &\triangleq \arg\max_{s\in\mathcal{X}} \left\{ \left|r_0 - E\left[r_0|\hat{\alpha}_0, \hat{\phi}_0\right]\right|^2 + \left|r_1 - E\left[r_1|\hat{\alpha}_1, \hat{\phi}_1\right]\right|^2 \right\} \\ &= \left| r_0 - \frac{\rho\sqrt{E_s}\hat{\alpha}_0 s}{\sigma_{\hat{\alpha}}} e^{\left(-0.5\sigma_\varepsilon^2\gamma^2 + j\gamma^2\hat{\phi}_0\right)} \right|^2 + \left| r_1 - \frac{\rho\sqrt{E_s}\hat{\alpha}_1 s}{\sigma_{\hat{\alpha}}} e^{\left(-0.5\sigma_\varepsilon^2\gamma^2 + j\gamma^2\hat{\phi}_1\right)} \right|^2. \end{aligned} \tag{4.15}$$

This novel ML decision metric in the presence of CSI and CFO estimation error for

a two branch SIMO can be further generalized for a m-branch SIMO as

$$s \triangleq \arg\max_{s\in\mathcal{X}} \sum_{k=m}^{1} \left(\ln\left(Var\left[r_k|\hat{\alpha}_k,\hat{\phi}_k\right]\right) + \frac{\left|r_k - E\left[r_k|\hat{\alpha}_k,\hat{\phi}_k\right]\right|^2}{2Var\left[r_k|\hat{\alpha}_k,\hat{\phi}_k\right]} \right) \tag{4.16}$$

and for PSK modulations as

$$s \triangleq \arg\max_{s\in\mathcal{X}} \sum_{k=0}^{m-1} \left| r_k - \frac{\rho\sqrt{E_s}\hat{\alpha}_k s}{\sigma_{\hat{\alpha}}} e^{\left(-0.5\sigma_\varepsilon^2\gamma^2 + j\gamma^2\hat{\phi}_k\right)} \right|^2. \tag{4.17}$$

4.2.1 Convergence to Conventional Metric

Let us consider two new expressions $\zeta = \rho/\sigma_{\hat{\alpha}}$ and $\xi = e^{\left(-0.5\sigma_\varepsilon^2\gamma^2 + j\gamma^2\hat{\phi}_k\right)}$ for simple readability and understanding. We can rewrite the proposed metric in (4.17) as

$$\sum_{k=0}^{m-1} \left| r_k - \zeta\sqrt{E_s}\hat{\alpha}_k s\xi \right|^2. \tag{4.18}$$

Now let us consider the system where there is no CFO. The value of the estimated CAFO $\hat{\phi}_k$ in this case becomes zero and the correlation coefficient γ (between $\phi_k = 0$ and $\hat{\phi}_k = 0$) becomes 1. Thus the new metric becomes

$$\sum_{k=0}^{m-1} \left| r_k - \frac{\rho}{\sigma_{\hat{\alpha}}}\sqrt{E_s}\hat{\alpha}_k s \right|^2 \tag{4.19}$$

which is the same metric given by Tarokh et al. shown in (4.11). We further consider the case of a perfect channel estimator. Here $\hat{\alpha}_k = \alpha_k$, $\rho = 1$ and so $\zeta = 1$, which reduces the proposed metric in (4.17) to the form discussed in (2.6) for perfect channel estimate and in the absence of CFO. This verifies that the new proposed metric is a generalized form and the conventional metrics are its special cases.

4.3 Linear Combiner

Linear Combiners and its types is explained elaborately in section 2.2. It is shown that among all types, MRC provides the most optimal solution in terms of maximizing the output SNR when the channel and the CFO are known to the receiver. From the expression of the baseband received signal in (4.3), let us consider a new expression

$$z_k = \alpha_k e^{j\phi_k} \tag{4.20}$$

for the k-th receive antenna. In practice, the receiver has the estimated value $\hat{z}_k = \hat{\alpha}_k e^{j\hat{\phi}_k}$ where $\hat{\alpha}_k$ is the channel estimate and $\hat{\phi}_k$ is the CAFO estimate. Thus the combiner in (3.11) can be written as

$$\hat{s} = \hat{z}_0^* r_0 + \hat{z}_1^* r_1 \tag{4.21}$$

and the ML detection cost function in (3.12) becomes

$$s \triangleq \arg\min_s \left\{ \left(|\hat{z}_0|^2 + |\hat{z}_1|^2 - 1 \right) |s|^2 + d^2 \left(\hat{s}, s \right) \right\}. \tag{4.22}$$

4.3.1 Combiner Design Methodology

The general form for a linear combiner for a two branch SIMO can be given as

$$\hat{s} = W^H R = W^H Z s + W^H N \tag{4.23}$$

where $W = [w_0 \quad w_1]^T$ are the combining weights or coefficients, $R = [r_0 \quad r_1]^T$, $Z = [z_0 \quad z_1]^T$ and $N = [n_0 \quad n_1]^T$. Here, we consider the case of Z unknown to the receiver and thus its optimum value is taken to be $Z_{opt} = E\left[Z | \hat{\alpha}, \hat{\phi} \right]$. The instantaneous output SNR of the combiner is given by

$$\Gamma = \frac{E\left[\left| W^H Z s \right|^2 \right]}{E\left[\left| W^H N \right|^2 \right]} = \frac{\sigma_s^2 \left| W^H E\left[Z | \hat{\alpha}, \hat{\phi} \right] \right|^2}{\sigma_n^2 \left\| W \right\|^2}. \tag{4.24}$$

By the Cauchy-Schwarz inequality, it is shown that the SNR Γ is maximum when $W = E\left[Z|\hat{\alpha},\hat{\phi}\right]$. Thus, using this result in (4.23), we get the new MRC for a two branch SIMO as

$$\hat{s} = \left(E\left[z_0|\hat{\alpha}_0,\hat{\phi}_0\right]\right)^* r_0 + \left(E\left[z_1|\hat{\alpha}_1,\hat{\phi}_1\right]\right)^* r_1. \tag{4.25}$$

We assume that the CSI α_k and the CAFO ϕ_k are independent of each other. Thus using the results from Appendix A, we can write

$$\begin{aligned} E\left[z_k|\hat{\alpha}_k,\hat{\phi}_k\right] &= E\left[\alpha_k e^{j\phi_k}|\hat{\alpha}_k,\hat{\phi}_k\right] \\ &= \frac{\rho\hat{\alpha}_k}{\sigma_{\hat{\alpha}}} e^{\left(-0.5\sigma_\varepsilon^2\gamma^2 + j\gamma^2\hat{\phi}_k\right)}. \end{aligned} \tag{4.26}$$

Substituting the value in (4.25), the new MRC for a two branch SIMO is

$$\hat{s} = \frac{\rho e^{\left(-0.5\sigma_\varepsilon^2\gamma^2\right)}}{\sigma_{\hat{\alpha}}} \left(\hat{\alpha}_0^* e^{\left(-j\gamma^2\hat{\phi}_0\right)} r_0 + \hat{\alpha}_1^* e^{\left(-j\gamma^2\hat{\phi}_1\right)} r_1\right). \tag{4.27}$$

The new MRC can be generalized for the case of m-branch SIMO

$$\hat{s} = \frac{\rho e^{\left(-0.5\sigma_\varepsilon^2\gamma^2\right)}}{\sigma_{\hat{\alpha}}} \sum_{k=0}^{m-1} \hat{\alpha}_k^* e^{\left(-j\gamma^2\hat{\phi}_k\right)} r_k. \tag{4.28}$$

4.3.2 ML Detection Methodology

The new ML detection cost function in the presence of estimation errors at the receiver is to choose s that minimizes

$$\left(\left|E\left[z_0|\hat{\alpha}_0,\hat{\phi}_0\right]\right|^2 + \left|E\left[z_1|\hat{\alpha}_1,\hat{\phi}_1\right]\right|^2 - 1\right)|s|^2 + d^2\left(\hat{s},s\right). \tag{4.29}$$

Using the results from (4.26), it can be written of the form

$$\left(|K\hat{\alpha}_0|^2 + |K\hat{\alpha}_1|^2 - 1\right)|s|^2 + d^2\left(\hat{s},s\right) \tag{4.30}$$

where

$$K = \frac{\rho e^{\left(-0.5\sigma_\varepsilon^2\gamma^2\right)}}{\sigma_{\hat{\alpha}}}.$$

For PSK constellations with equal energy, the ML cost function remains $d^2\left(\hat{s},s\right)$.

4.3.3 Convergence to Conventional MRC

The conventional MRC given in (2.16), assumes that the both the CSI and CFO are known to the receiver. Let us assume a similar case for the new derived MRC which means, both the estimators of the CSI and CFO at the receiver are perfect i.e. $\hat{\alpha}_k = \alpha_k$ and $\hat{\phi}_k = \phi_k$. The correlation coefficient between the original CSI α_k and its estimate $\hat{\alpha}_k$, $\rho = 1$. Similarly for CAFO, the correlation coefficient between ϕ_k and $\hat{\phi}_k$, $\gamma = 1$. Substituting these values in (4.28) and (4.30), $\rho e^{\left(-0.5\sigma_\varepsilon^2\gamma^2\right)}/\sigma_{\hat{\alpha}} = 1$ and we get the form of the conventional MRC with known CSI and CFO which is

$$\hat{s} = \sum_{k=0}^{m-1} \alpha_k^* e^{(-j\phi_k)} r_k \tag{4.31}$$

and the conventional ML detector given in (2.19) respectively. Thus, it can be shown that the new derived combiner can be reduced to the conventional MRC for the ideal case of perfect CSI and CFO estimators.

4.4 L-MMSE

Linear MMSE detectors described in section 2.3, are designed to minimize the mean square error between the transmitted signal and one obtained after detection. A generalized linear estimator can be written in the form

$$\hat{s} = KR, \tag{4.32}$$

where $\hat{s}$ is the signal after detection, $R = [r_0 \;\; r_1]^T$ are the received signals and $K = [K_0 \;\; K_1]$ are the coefficients of the detector. By, Orthogonality principle explained earlier, the mean square error can be minimized when

$$\begin{aligned} & (s - \hat{s}) \perp R \\ \Rightarrow\; & E\left[(s - \hat{s})\, R^H\right] = 0 \\ \Rightarrow\; & E\left[(s - KR)\, R^H\right] = 0. \end{aligned} \tag{4.33}$$

The system in this scenario does not have the knowledge of the CSI and CFO. Thus, the imperfect estimates of CSI $\hat{\alpha}_k$ and CAFO $\hat{\phi}_k$ are available to the receiver. Let us assume

$$\hat{z}_k = \hat{\alpha}_k e^{j\hat{\phi}_k} \tag{4.34}$$

and $\hat{Z} = [\hat{z}_0 \;\; \hat{z}_1]^T$. From (4.33), in the presence of estimation errors, the mean square error can be minimized by

$$\begin{aligned} & E\left[(s - KR)\, R^H \,\middle|\, \hat{Z}\right] = 0 \\ \Rightarrow\; & E\left[sR^H \,\middle|\, \hat{Z}\right] - KE\left[RR^H \,\middle|\, \hat{Z}\right] = 0 \\ \Rightarrow\; & K = E\left[sR^H \,\middle|\, \hat{Z}\right] E\left[RR^H \,\middle|\, \hat{Z}\right]^{-1}. \end{aligned} \tag{4.35}$$

Calculating these parameters individually,

$$E\left[RR^H\right] = E\left[\left[\begin{array}{c} r_0 \\ r_1 \end{array}\right]\left[\begin{array}{cc} r_0 & r_1 \end{array}\right]^* \middle| \hat{Z}\right]$$

$$= \left[\begin{array}{cc} \sigma_s^2 E\left[|z_0|^2 \middle| \hat{\alpha}_0, \hat{\phi}_0\right] + \sigma_n^2 & 0 \\ 0 & \sigma_s^2 E\left[|z_1|^2 \middle| \hat{\alpha}_1, \hat{\phi}_1\right] + \sigma_n^2 \end{array}\right] \tag{4.36}$$

$$\Rightarrow\; E\left[RR^H\right]^{-1} = \left[\begin{array}{cc} \dfrac{1}{\sigma_s^2 E\left[|z_0|^2 \middle| \hat{\alpha}_0, \hat{\phi}_0\right] + \sigma_n^2} & 0 \\ 0 & \dfrac{1}{\sigma_s^2 E\left[|z_1|^2 \middle| \hat{\alpha}_1, \hat{\phi}_1\right] + \sigma_n^2} \end{array}\right].$$

Similarly, we calculate

$$\begin{aligned} E\left[sR^H\right] &= E\left[\left[\begin{array}{cc} sr_0^* & sr_1^* \end{array}\right] \middle| \hat{Z}\right] \\ &= \sigma_s^2 \left[\begin{array}{cc} \left(E\left[z_0 | \hat{\alpha}_0, \hat{\phi}_0\right]\right)^* & \left(E\left[z_1 | \hat{\alpha}_1, \hat{\phi}_1\right]\right)^* \end{array}\right]. \end{aligned} \tag{4.37}$$

Substituting, the values from (4.36) and (4.37) in (4.35), the coefficients of MMSE detector becomes

$$K = \left[\underbrace{\frac{\sigma_s^2 \left(E\left[z_0 | \hat{\alpha}_0, \hat{\phi}_0 \right] \right)^*}{\sigma_s^2 E\left[|z_0|^2 \middle| \hat{\alpha}_0, \hat{\phi}_0 \right] + \sigma_n^2}}_{K_0} \quad \underbrace{\frac{\sigma_s^2 \left(E\left[z_1 | \hat{\alpha}_1, \hat{\phi}_1 \right] \right)^*}{\sigma_s^2 E\left[|z_1|^2 \middle| \hat{\alpha}_1, \hat{\phi}_1 \right] + \sigma_n^2}}_{K_1} \right]. \tag{4.38}$$

All elaborate calculations are shown in Appendix A, which gives us the value of

$$E\left[z_k | \hat{\alpha}_k, \hat{\phi}_k \right] = \frac{\rho \hat{\alpha}_k}{\sigma_{\hat{\alpha}}} e^{\left(-0.5\sigma_{\varepsilon}^2 \gamma^2 + j\gamma^2 \hat{\phi}_k \right)} \tag{4.39}$$

and

$$E\left[|z_k|^2 \middle| \hat{\alpha}_k, \hat{\phi}_k \right] = 1 - \rho^2 + \frac{\rho^2 \left| \hat{\alpha}_k \right|^2}{\sigma_{\hat{\alpha}}^2}. \tag{4.40}$$

Thus from (4.32), the novel optimal linear MMSE detector for a two branch SIMO in the presence of CSI and CFO estimation errors is

$$\hat{s} = K_0 r_0 + K_1 r_1 \tag{4.41}$$

and for m-branch SIMO systems, it becomes

$$\hat{s} = \sum_{k=0}^{m-1} K_k r_k. \tag{4.42}$$

4.4.1 Convergence to Conventional L-MMSE

Ideal systems are considered to have perfect channel estimators and no CFO. The conventional MMSE derived in section 2.3, is for such an ideal case. Here, we consider two special cases for the novel MMSE detector derived above.

1. **Perfect CSI and CFO estimator**: Here we assume that the estimator for both CSI and CFO are perfect i.e. $\hat{\alpha}_k = \alpha_k$ and $\hat{\phi}_k = \phi_k$ respectively. This makes the values of the respective correlation coefficients unity i.e. $\rho = \gamma = 1$. It is evident now, that the variances of the CSI and CFO estimates are $\sigma_{\hat{\alpha}}^2 = \sigma_{\alpha}^2$

and $\sigma^2_{\hat{\phi}} = \sigma^2_{\phi}$ respectively. Substituting these values in (4.41), we get

$$\hat{s} = \sum_{k=0}^{m-1} \frac{\sigma_s^2 \ \alpha_k^* \ e^{-j\phi_k} \ r_k}{\sigma_s^2 \left|\alpha_k\right|^2 + \sigma_n^2} \tag{4.43}$$

which is the form of conventional MMSE detector in the presence of perfect estimation at the receiver.

2. **Perfect CSI estimator and no CFO**: Let us make the similar assumption as above. However, now we assume a system in the absence of CFO. This means $\hat{\phi}_k = \phi_k = 0$, $\sigma^2_{\hat{\phi}} = \sigma^2_{\phi} = 0$ and $\gamma = 1$. Thus, the MMSE detector in (4.43) becomes

$$\hat{s} = \sum_{k=0}^{m-1} \frac{\sigma_s^2 \ \alpha_k^* \ r_k}{\sigma_s^2 \left|\alpha_k\right|^2 + \sigma_n^2}. \tag{4.44}$$

This is the form of a conventional MMSE detector for an ideal scenario.

Thus, it is shown that the proposed MMSE detection algorithm is a general form for practical systems and the conventional algorithms are its special cases.

Chapter 5

Simulation and Performance Analysis

In this section, we analyze the efficiency demonstrated by the new detection algorithms proposed in section 4. The simulation is performed for a two branch SIMO system as described in a block diagram given in Fig. 2.1, with a single transmit antenna and two receive antennas.

The simulations are performed for a flat Rayleigh fading channel and its parameters are assumed to follow standard normal distribution. As discussed earlier, the channel estimates assume the form given in (3.2). We have considered a linear MMSE channel estimator where, the estimation error is a function of AWGN variance and pilot length as given in (3.15). The length of the pilot symbols is assumed to be 16, for all the simulations shown in this section. The original CFO is taken as a zero mean Gaussian RV. The imperfect estimate of CFO is of the form given in (3.17) where the estimation error is also considered to follow Gaussian distribution. The variance of the CFO estimation error is considered a multiple of the AWGN variance and simulations are performed for three different values of the error variance. This is done, to demonstrate the performance of the proposed algorithms for high values of CFO estimation error.

Performance analysis is done by plotting BER against the SNR. Complex data symbols are considered for the simulation and total of 10^4 frames are transmitted for each value of SNR with a frame length of 130 symbols. The simulations are performed for different modulation schemes of 4, 16 and 64 QAM and also 4, 8 and 16 PSK for the case of equal energy constellation. The AWGN variance N_0 depends on the SNR Γ and the modulation scheme.

$$\begin{aligned} \Gamma &= \frac{E_b}{N_0} \\ &= \frac{E_s}{R_m R_c N_0} \end{aligned} \tag{5.1}$$

$$\Rightarrow \; N_0 = \frac{E_s}{R_m R_c \Gamma},$$

where E_s is the symbol energy, $R_m = \log_2(M)$ for M-ary modulation scheme and R_c is the code rate of the system. For modulation schemes having equal energy constellations like PSK, $E_s = 1$. Here, we assume no coding for the system and so $R_c = 1$.

5.1 Proposed ML Detector

This section demonstrates the simulation method and results of the ML detector metric proposed in section 4.2. The new metric in the presence of channel and CFO estimation error is compared with the conventional metric. The conventional metric proposed by Tarokh et.al [51] was derived in the presence of channel estimation error and is prevalently used in present day MIMO systems [77]. Fig. 5.1 shows, the performance simulation for 4-PSK modulation scheme and Fig. 5.2 shows the simulation for 8-PSK and 16-PSK modulation schemes.

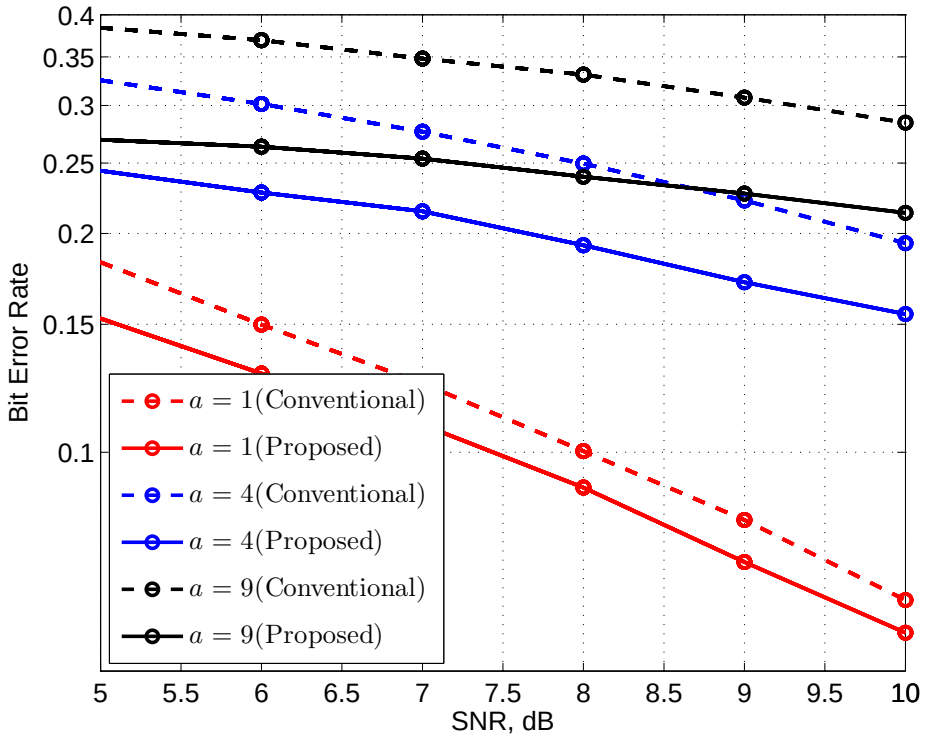

Figure 5.1: Proposed ML detection metric with 4-PSK modulation

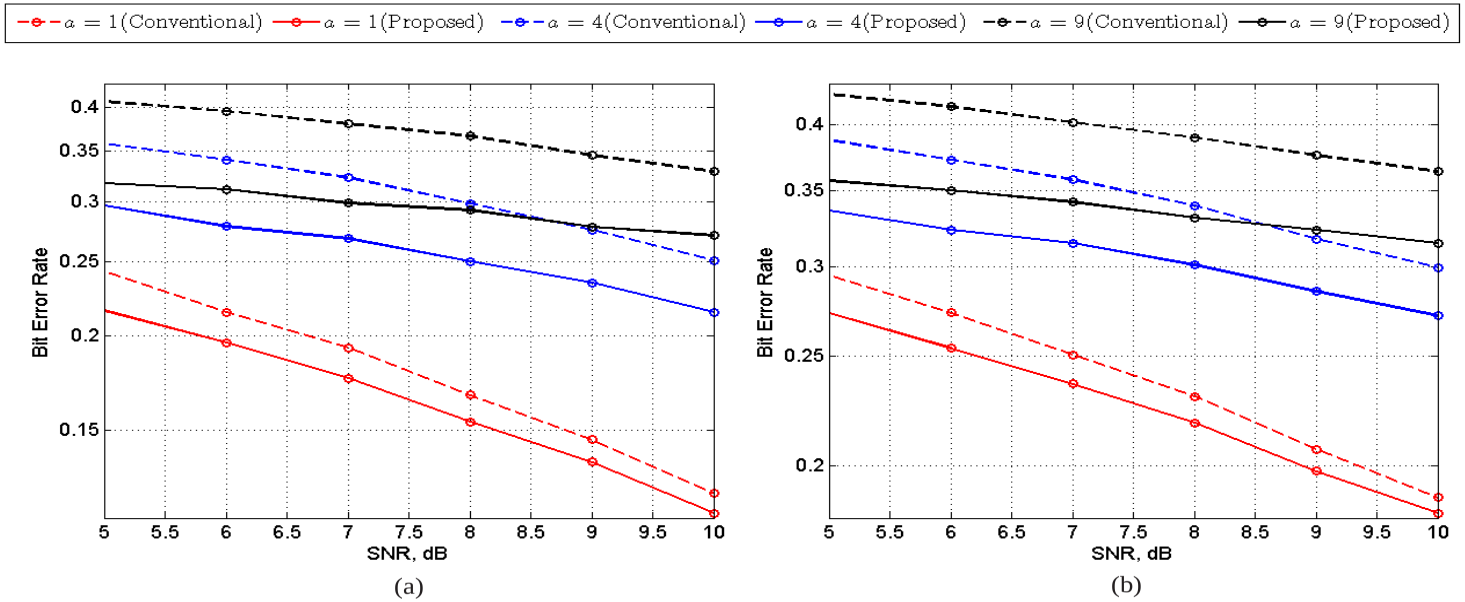

Figure 5.2: Performance simulation of proposed ML detector for

(a) 8-PSK modulation (b) 16-PSK modulation

It is shown that for a system with unknown CSI and CFO provides more than 5-dB gain in SNR over the conventional metric for a given BER. The value of the gain is higher for high CFO estimation error variance. The performance of the proposed metric elevates also for high modulation schemes. Fig. 5.3 demonstrates the performance for 4-QAM, for which the proposed metric also provides over 5-dB gain. It can be seen in Fig. 5.4 that the performance of the whole system deteriorates for 16-QAM and 64-QAM as the modulation maps 4 and 16 symbols in each constellation. However, the proposed metric provides better results in terms of BER.

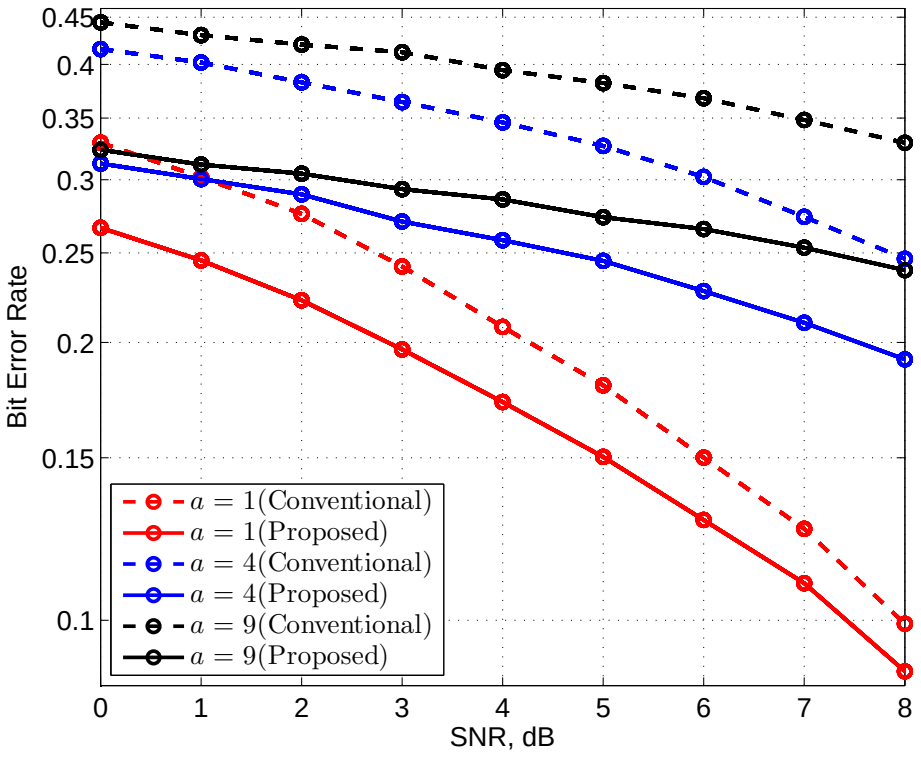

Figure 5.3: Proposed ML detection metric with 4-QAM modulation

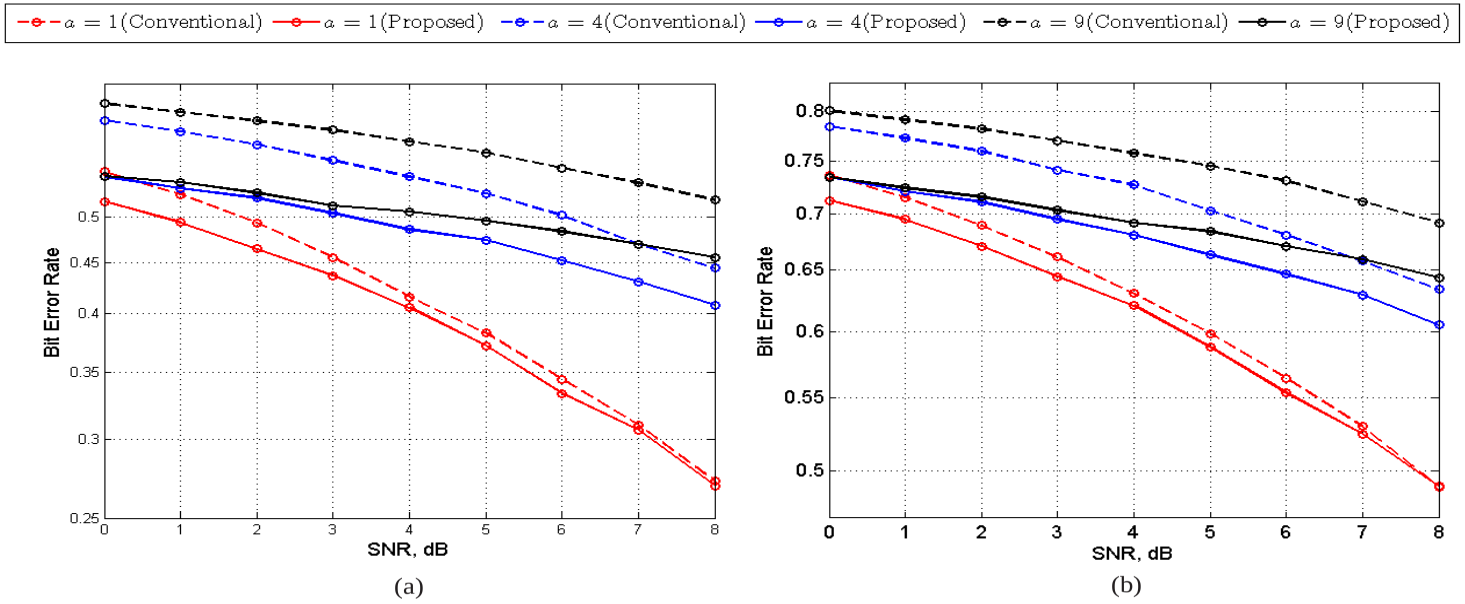

Figure 5.4: Performance simulation of proposed ML detector for

(a) 16-QAM modulation (b) 64-QAM modulation

5.2 Proposed Linear Combiner

This section, demonstrates the performance of the proposed MRC for a system with imperfect estimates of CSI and CFO. The proposed MRC provides optimal solution with maximum output SNR after combining. The performance is compared with the classical form of MRC given in section 3.2.2 known for ideal systems. The output of the MRC is further fed into a ML detector to minimize the BER. Fig. 5.5 shows the simulation of the proposed MRC and ML compared to their classical form for 4-PSK modulation. The simulation is performed for multiple values of estimation error variances and higher modulation schemes 8-PSK and 16-PSK in Fig 5.6.

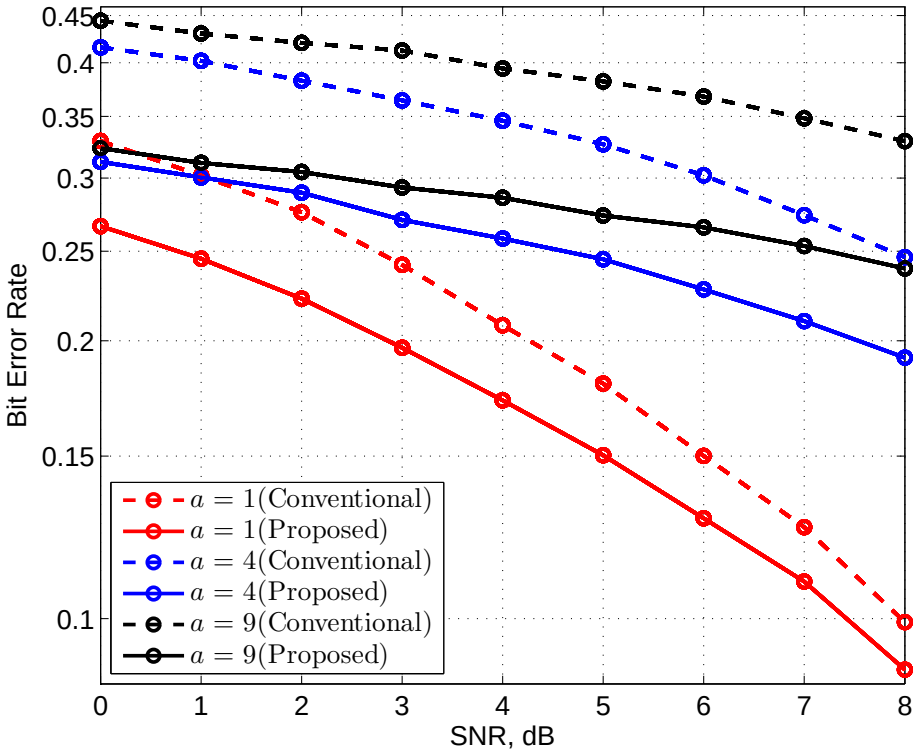

Figure 5.5: Proposed linear combiner with 4-PSK modulation

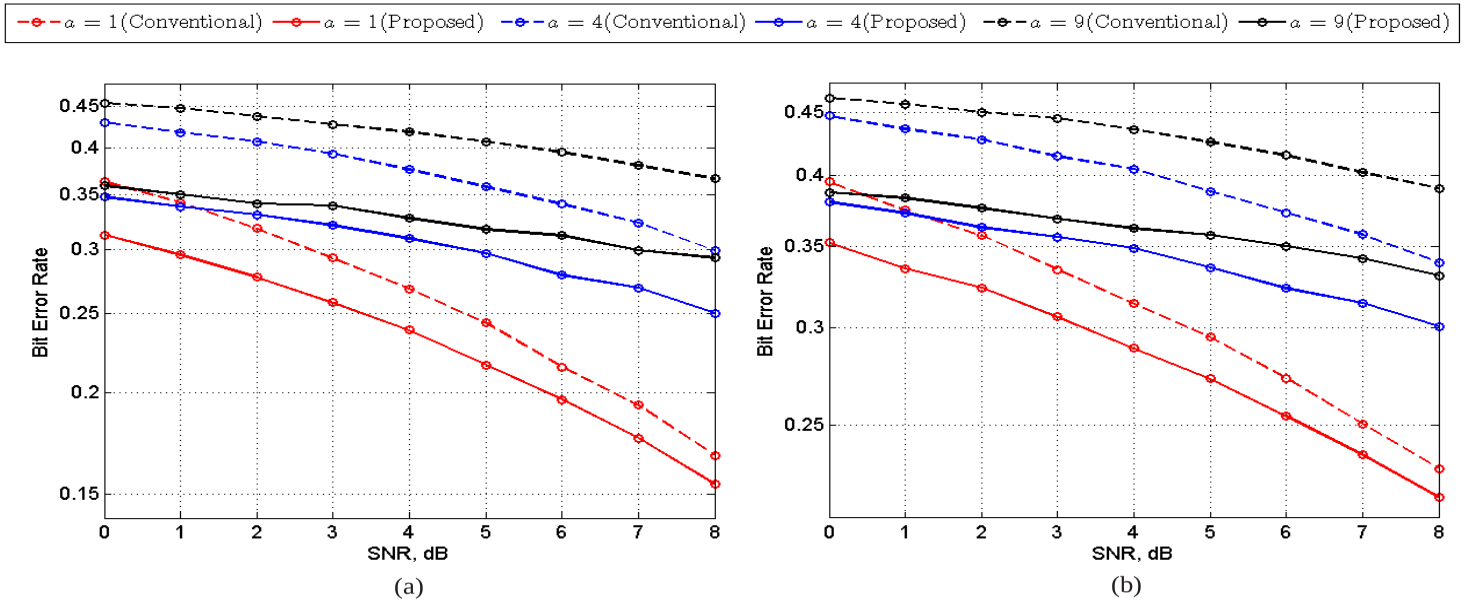

Figure 5.6: Performance simulation of proposed linear combiner for

(a) 8-PSK modulation (b) 16-PSK modulation

The proposed MRC and ML detector demonstrate over 5-dB gain as compared to the classical model under the mismatch scenario. For, higher PSK modulation schemes, it outperforms the classical model by much higher gain in SNR. It is obvious from the simulation results that the combiner provides better gain for high estimation error. Fig. 5.7 is the simulation result with 4-QAM modulation. The performance is identical to that of 4-PSK, as both the schemes map only one symbol per constellation. Fig. 5.8 shows the performance for 16-QAM and 64-QAM. When compared with the performance of the proposed ML detector shown in section 5.1, the new linear combiner demonstrates identical performance.

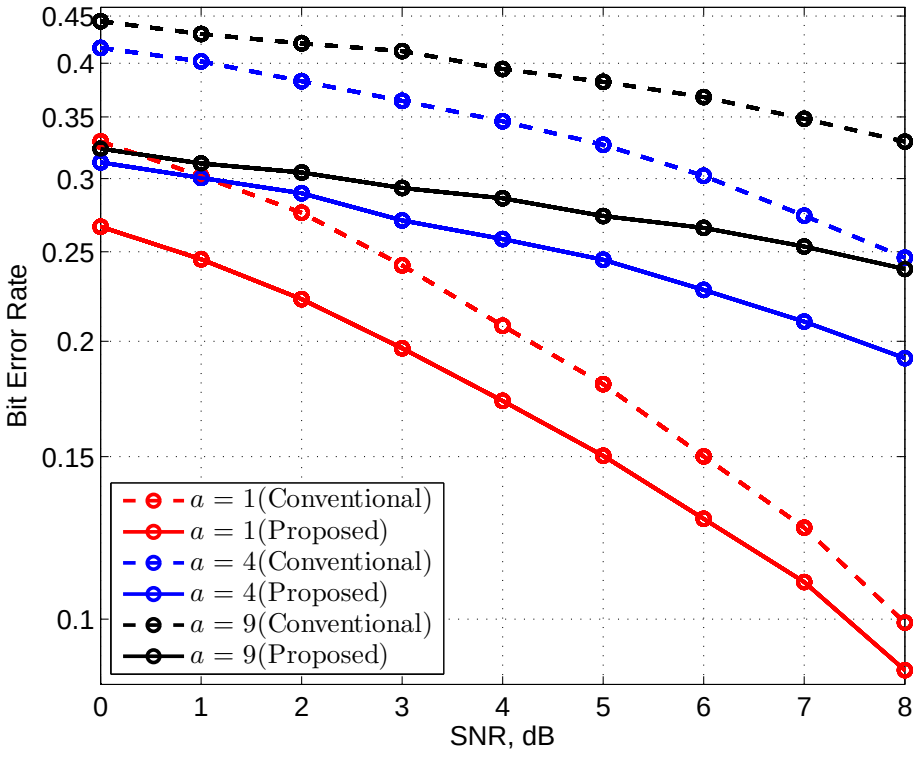

Figure 5.7: Proposed linear combiner with 4-QAM modulation

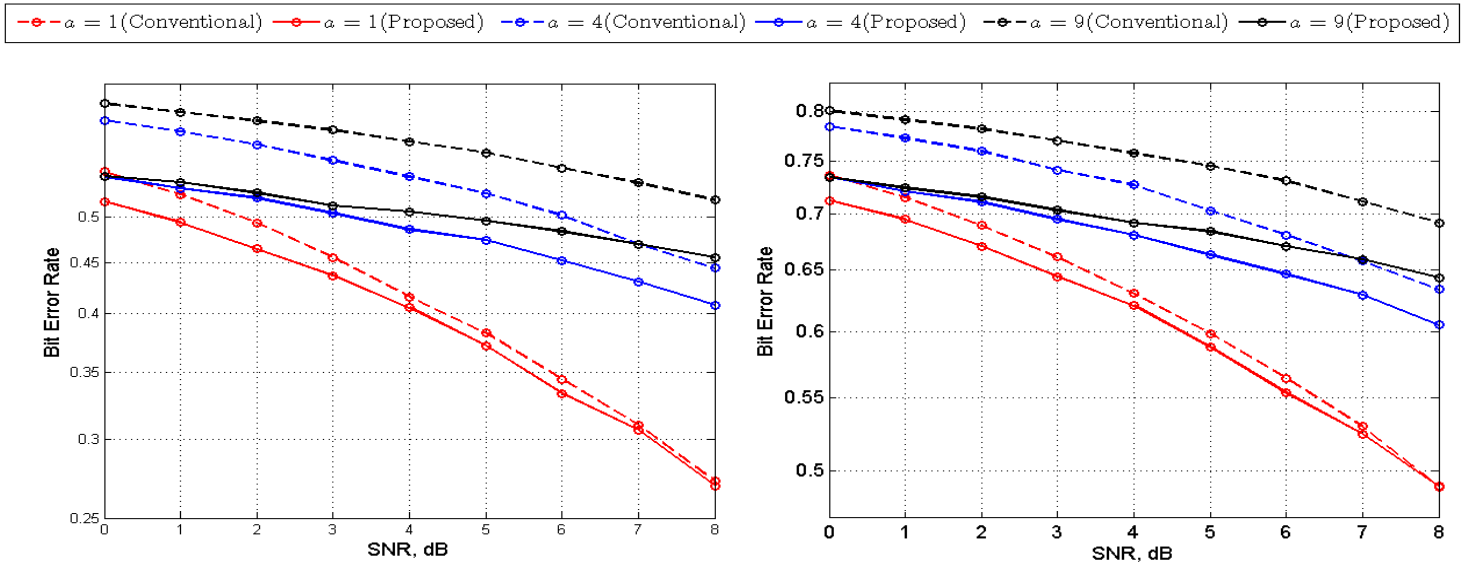

Figure 5.8: Performance simulation of proposed linear combiner for

(a) 16-QAM modulation (b) 64-QAM modulation

5.3 Proposed L-MMSE Detector

Linear MMSE estimators are one of the classical low complexity linear estimation models that provides optimal solution in terms of minimizing its output error. Here, the performance of the proposed detector in section 4.4, based on this model is compared with the classical L-MMSE given in 3.2.3 for CSI and CFO mismatch scenario. As shown in the previous sections, the efficiency of the proposed detector is simulated 4-PSK modulation in Fig 5.9. Furthermore, the BER plot against different values of the SNR is also shown for 8-PSK and 16-PSK modulation schemes in Fig. 5.10.

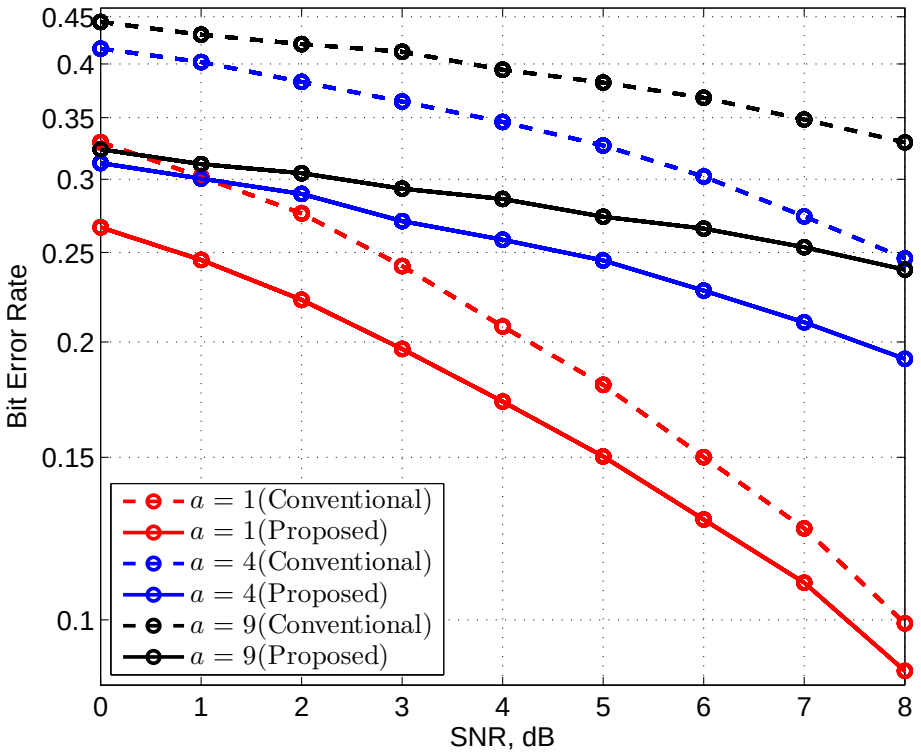

Figure 5.9: Proposed L-MMSE with 4-PSK modulation

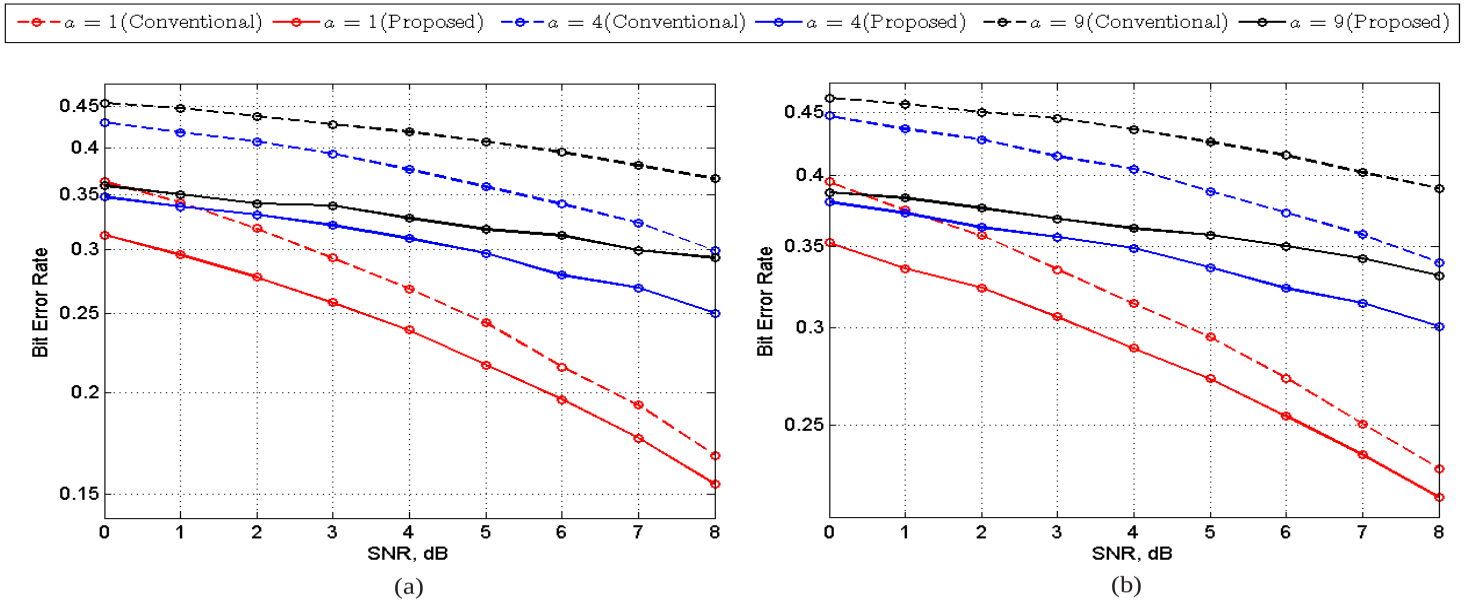

Figure 5.10: Performance simulation of proposed L-MMSE for

(a) 8-PSK modulation (b) 16-PSK modulation

The proposed linear detector provides above 5-dB gain for the value CFO estimation error variance as 9 times the AWGN variance. The performance of the proposed L-MMSE detector is identical to the performance of two algorithms shown in the previous sections. The BER verses SNR curve is also plotted for 4-QAM, 16-QAM and 64-QAM in Fig. 5.11 and Fig. 5.12 respectively. The performance of the whole system degrades for higher modulation schemes. However, the proposed metric demonstrates improved performance for high modulation index and high values of estimation error variance.

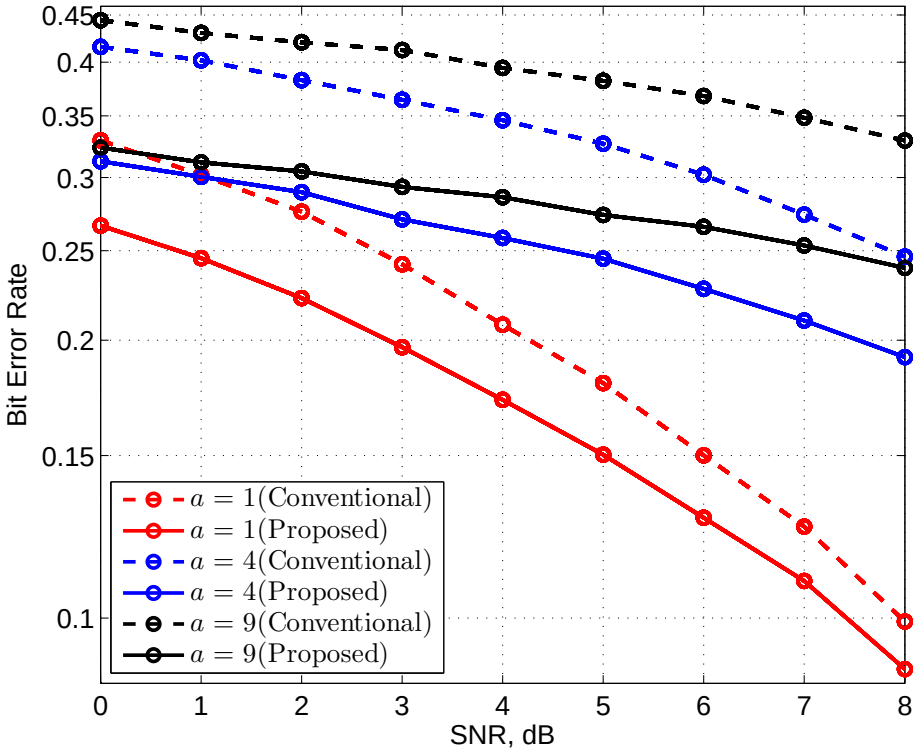

Figure 5.11: Proposed L-MMSE with 4-QAM modulation

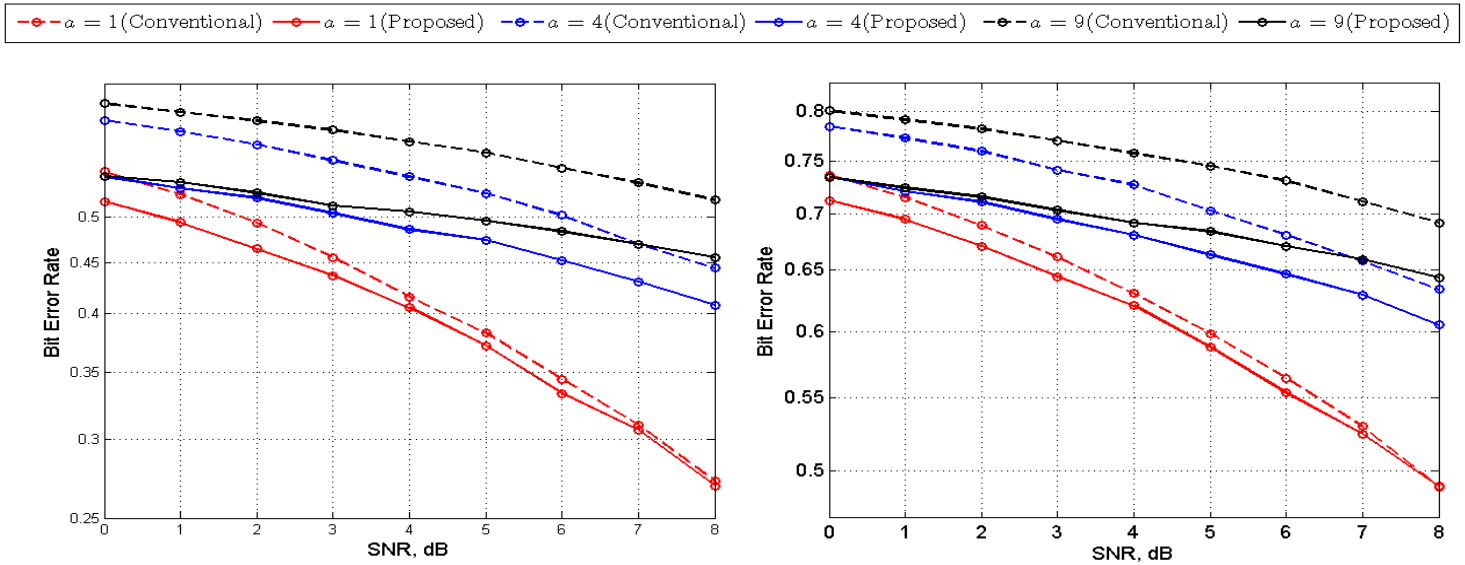

Figure 5.12: Performance simulation of proposed L-MMSE for

(a) 16-QAM modulation (b) 64-QAM modulation

The simulation results presented above for all three proposed detection algorithms demonstrate significant improvement in terms of BER as compared to their respective conventional detectors. The main focus of the simulation was to demonstrate the performance with various values of the CFO estimation error variance. It is evident from the simulation diagrams, that the gain in SNR provided by the proposed algorithms increases with higher values of the estimation error. Apart from that, for lower values of SNR, i.e. for the case of low signal strength, the algorithms have comparatively lower BER than the conventional forms and it is visible that the gap increases for increasing estimation error.

Let us now analyze the computation complexity of each of these detectors. Firstly, the ML detector operates by choosing an appropriate symbol from a given set to minimize a metric. This process involves multiple iterations and the total computation time is unknown. The second detector involves two blocks, one is a linear combiner which has the same complexity as a linear estimator and second, is a ML detection block which again has a comparatively high computation time and complexity. The third detection algorithm is a linear MMSE detector which is the most general form of a linear estimator has the least complexity in terms of time and cost among all the other techniques presented here.

It is also observed from the simulation diagrams, that the performance of all the three proposed detectors are identical in terms of BER. With this observation, the following inferences can be made:

1. All the three proposed detection algorithms provide optimal detection in terms of BER under CSI and CFO mismatch scenario.

2. The Gaussian approximation made during derivation of the proposed ML detector in the presence of CFO is appropriate, as it provides an optimal performance.

3. The implementation and time complexity of L-MMSE being the least among the other two detectors, makes it the best choice for practical implementation.

Chapter 6

Conclusion and Future Work

This thesis addresses the unexploited challenges faced by a practically implemented WC system. The cases of both multi-channel fading and CFO are taken in consideration. Motivated by the shortcomings of the existing detection techniques, this work delivers an optimal solution for detection of the transmitted signal in the presence of channel and CFO estimation error.

The proposed algorithms aim to augment three different, prevalent detection techniques that are used practically. The first proposed approach involves the classical ML detection method. A metric is proposed for a system, incorporating unknown channel parameters and CFO. The performance of this metric is compared with the conventional metric widely used for MIMO systems. The second detection method is based on linear combining technique and is optimal in the sense of maximizing the output SNR. This also includes derivation of another ML detection metric to minimize the BER of the combiner output. The third proposed method exploits the ubiquitous linear MMSE detection technique, which provides an optimal solution for minimizing the error. It is also shown mathematically that for ideal cases with perfect knowledge of channel and CFO, the proposed algorithms generalize and converge to their respective classical forms.

The proposed algorithms are primarily derived for a two branch SIMO system with one transmit and two receive antenna, and are further extended for the general case of multiple m-receive antennas. The performance of these detection algorithms is analyzed using simulation and plotting BER against the SNR. The simulation is performed for 4, 16 and 64 QAM modulation schemes along with equal energy modulation schemes such as 4, 8 and 16 PSK. A performance comparison is made with the conventional forms of these detection techniques. It is shown that the proposed algorithms demonstrate significant improvement under the mismatch channel and CFO scenario. Simulation results also validate its capacity to deal with very high estimation errors and the performance is shown to improve with the increase of estimation error variance. Thus, it can be concluded that the detection algorithms proposed in this thesis are a novel approach for practical implementation.

The system model considered in this thesis is a simple general case of a MIMO system. The work presented here, can be further extended for more complicated cases such as multi-user MIMO systems or different modulation schemes such as OFMA used in LTE, where mitigation of CFO is a crucial challenge. Apart from that, similar approach for deriving detection algorithms conditioned on imperfect estimates can be adapted for various other detection techniques used practically. Addressing these two avenues can be considered for future enhancement of this research project.

References

[1] W. Weaver, "The mathematics of communication," *Scientific American*, vol. 181, no. 1, pp. 11–15, July 1949.

[2] C.E. Shannon, "Communication in the presence of noise," *Proceedings of the IRE*, vol. 37, no. 1, pp. 10–21, Jan. 1949.

[3] N. Srivastava, "Diversity schemes for wireless communication-a short review," *J. Theoritical and Appl. Info. Tech.*, vol. 15, no. 2, pp. 134–143, May 2010.

[4] M.K. Simon and M. Alouini, "A unified approach to the performance analysis of digital communication over generalized fading channels," *in Proc. IEEE*, vol. 86, no. 9, pp. 1860–1877, Sept. 1998.

[5] D.G. Brennan, "On the maximal signal-to-noise ratio realizable from several noisy signals," *Proc. IRE*, vol. 43, no. 10, pp. 1530, 1955.

[6] D.G. Brennan, "Linear diversity combining techniques," *Proc. IRE*, vol. 47, pp. 1075–1102, Jun 1959.

[7] W.C. Jakes, "Microwave mobile communications," *Wiley, New York*, 1974.

[8] R.A. Monzingo and T.W. Miller, "Introduction to adaptive arrays," *Wiley, New York*, 1980.

[9] H. Jafarkhani, "Space-time coding: Theory and practice," *Cambridge University Press*, 2005.

[10] V. Weerackody, "Diversity for direct-sequence spread spectrum using multiple transmit antennas," *in Proc. IEEE Int. Commun. Conf.*, pp. 1775–1779, May 1993.

[11] S.M. Alamouti, "A simple transmit diversity technique for wireless communications," *IEEE J. Select. Areas Commun.*, vol. 16, no. 8, pp. 1451–1458, Oct 1998.

[12] V. Tarokh, H. Jafarkhani, and A.R. Calderbank, "Space-time block codes from orthogonal designs," *IEEE Trans. Info. Theory*, vol. 45, no. 5, pp. 1456–1467, July 1999.

[13] B. Hochwald, T.L. Marzetta, and C.B. Papadias, "A transmitter diversity scheme for wideband CDMA systems based on space-time spreading," *IEEE J. Select. Areas Commun.*, vol. 19, no. 1, pp. 48–60, Jan. 2001.

[14] J. Mietzner, R. Schober, L. Lampe, W.H. Gerstacker, and P.A. Hoeher, "Multiple-antenna techniques for wireless communications - a comprehensive literature survey," *IEEE Commun. Surveys Tutorials*, vol. 11, no. 2, pp. 87–105, June 2009.

[15] J.H. Winters, J. Salz, and R.D. Gitlin, "The impact of antenna diversity on the capacity of wireless communication systems," *IEEE Trans. Commun.*, vol. 42, no. 234, pp. 1740 –1751, Feb. 1994.

[16] S. Sharma, "Communication systems (analog and digital)," *S K Kataria and sons*, 2009.

[17] G. Forney Jr., R. Gallager, G. Lang, F. Longstaff, and S. Qureshi, "Efficient modulation for band-limited channels," *IEEE J. Select. Areas Commun.*, vol. 2, no. 5, pp. 632–647, Sept. 1984.

[18] B.P. Lathi and Z. Ding, "Modern digital and analog communication systems," *Oxford University Press*, 2009.

[19] M. Kumar, S. Tripathi, A. Vidyarathi, S. Mohanty, and R. Gowri, "Various psk modulation schemes for wireless communication," *in Proc. IEEE Int. Comp. Commun. Tech. (ICCCT)*, pp. 545–549, Sept. 2011.

[20] C. Tellambura, A.J. Mueller, and V.K. Bhargawa, "Analysis of M-ary phase-shift keying with diversity reception for land-mobile satellite channels," *IEEE Trans. on Vehicular Tech.*, vol. 46, no. 4, pp. 910–922, Nov. 1997.

[21] T. Le-Ngoc, G.M. Lieu, and V.K. Bhargava, "Performance of M-ary QAM schemes in a line-of-sight multipath fading channel," *in Proc. IEEE Pacific RIM Commun. Computers and Signal Process.*, pp. 396–399, June. 1989.

[22] K. Yu, J.S. Evans, and I.B. Collings, "Performance analysis of LMMSE receivers for M-ary QAM in rayleigh faded CDMA channels," *IEEE Trans. on Vehicular Tech.*, vol. 52, no. 5, pp. 1242–1253, Sept. 2003.

[23] H. Bai and M. Atiquzzaman, "Error modeling schemes for fading channels in wireless communications: A survey," *IEEE Commun. Surveys Tutorials*, vol. 5, no. 2, pp. 2–9, Quarter. 2003.

[24] R.D. Yates and D.J. Goodman, "Probability and stochastic processes a friendly introduction for electrical and computer engineers," *John Wiley and Sons, Inc.*, 2005.

[25] J. Aruz, P. Krishnamurthy, and M. A. Labrador, "Discrete rayleigh fading channel modeling," *Wirel. Commun. Mob. Comput.*, vol. 4, no. 4, pp. 413–425, June 2004.

[26] P.A. Dighe, R.K. Mallik, and S.S. Jamuar, "Analysis of transmit-receive diversity in rayleigh fading," *IEEE Trans. Commun.*, vol. 51, no. 4, pp. 694–703, April 2003.

[27] M.O. Hasna and M.S. Alouini, "End-to-end performance of transmission systems with relays over rayleigh-fading channels," *IEEE Trans. on Wireless Commun.*, vol. 2, no. 6, pp. 1126–1131, Nov. 2003.

[28] Z. Chen, J.Yuan, and B.Vucetic, "Analysis of transmit antenna selection/maximal-ratio combining in rayleigh fading channels," *IEEE Trans. on Vehicular Tech.*, vol. 54, no. 4, pp. 1312–1321, July. 2005.

[29] T. Xiaoyi, M.S. Alouini , and A.J. Goldsmith, "Effect of channel estimation error on M-QAM BER performance in rayleigh fading," *IEEE Trans. Commun.*, vol. 47, no. 12, pp. 1856–1864, Dec. 1999.

[30] F. Gini and G.B. Giannakis, "Frequency offset and symbol timing recovery in flat-fading channels: a cyclostationary approach," *IEEE Trans. Commun.*, vol. 46, no. 3, pp. 400–411, March 1998.

[31] K. Younsun, B. Keukjoon, C. Sooyong, Y. Cheolwoo, and H. Daesik, "Effect of carrier frequency offset on performance of MC-CDMA systems," *IEEE Electronics Letters.*, vol. 35, no. 5, pp. 378–379, March. 1999.

[32] H. Steendam and M. Moeneclaey, "The effect of carrier frequency offsets on downlink and uplink MC-DS-CDMA," *IEEE J. Select. Areas Commun.*, vol. 19, no. 12, pp. 2528–2536, Dec. 2001.

[33] L. Pan and Y. Bar-Ness, "Wlc43-4: Comparing the effect of carrier frequency offset on OFDM and single-carrier block transmission in AWGN channels," *in Proc. IEEE Global Telecommun.*, pp. 1–5, Dec. 2006.

[34] X. Ma, H. Kobayashi, and S.C. Schwartz, "Effect of frequency offset on BER of OFDM and single carrier systems," *in Proc. IEEE Pers. Indoor Mob. Radio Commun.*, vol. 3, pp. 2239–2243, Sept. 2003.

[35] P. Balaban and J. Salz, "Optimum diversity combining and equalization in digital data transmission with applications to cellular mobile radio. i. theoretical considerations," *IEEE Trans. Commun.*, vol. 40, no. 5, pp. 885–894, May 1992.

[36] L.C. Godara, "Applications of antenna arrays to mobile communications. i. performance improvement, feasibility, and system considerations," *in Proc. IEEE*, vol. 85, no. 7, pp. 1031–1060, July 1997.

[37] A. Semmar, J.Y. Chouinard, V.H. Pham, X. Wang, Y. Wu, and S. Lafleche, "Digital broadcasting television channel measurements and characterization for SIMO mobile reception," *IEEE Trans. Broadcast.*, vol. 52, no. 4, pp. 450–463, Dec. 2006.

[38] E.G. Larsson, "MIMO detection methods: How they work [lecture notes]," *IEEE Signal Processing Magazine*, vol. 26, no. 3, pp. 91–95, May 2009.

[39] J. Wang and B. Daneshrad, "A comparative study of mimo detection algorithms for wideband spatial multiplexing systems," *in Proc. IEEE Wireless Commun.and Network.*, vol. 1, pp. 408–413, March 2005.

[40] T. Wo, J.C. Fricke, and P.A. Hoeher, "A graph-based iterative gaussian detector for frequency-selective MIMO channels," *in Proc. IEEE Info. Theory Workshop, Punta del Este.*, pp. 581–585, Oct. 2006.

[41] X. Zhu and R.D. Murch, "Performance analysis of maximum likelihood detection in a MIMO antenna system," *IEEE Trans. Commun.*, vol. 50, no. 2, pp. 187–191, Feb. 2002.

[42] W. Peng, M. Shaodan, N. Tung-Sang, W. Jiangzhou, and F. Adachi, "Performance analysis on maximum likelihood detection for two input multiple output systems," *in Proc. IEEE Vehicular Tech.*, pp. 1–5, Sept. 2008.

[43] G.V.V. Sharma and A. Chockalingam, "Performance analysis of maximum-likelihood multiuser detection in space-time coded CDMA with imperfect channel estimation," *in Proc. IEEE Vehicular Tech.*, pp. 1664–1668, May. 2004.

[44] M. Kiessling, J. Speidel, N. Geng, and M. Reinhardt, "Performance analysis of MIMO maximum likelihood receivers with channel correlation, colored gaussian noise, and linear prefiltering," *in Proc. IEEE Intl. Conf. Commun.*, pp. 3026–3030, May. 2003.

[45] A. Shah and A.M. Haimovich, "Performance analysis of optimum combining in wireless communications with rayleigh fading and cochannel interference," *IEEE Trans. Commun.*, vol. 46, no. 4, pp. 473–479, April 1998.

[46] T. Eng, N. Kong, and L.B. Milstein, "Comparison of diversity combining techniques for rayleigh-fading channels," *IEEE Trans. Commun.*, vol. 44, no. 9, pp. 1117–1129, Sept. 1996.

[47] S.S. Dragomir, "A survey on cauchy-bunyakovsky-schwarz type discrete inequalities," *J. Ineq. Pure and Appl. Math.*, vol. 4, no. 3, pp. 63, May 2003.

[48] A.H. Sayed, "Fundamentals of adaptive filtering," *John Wiley and Sons, Inc.*, 2003.

[49] K. Namshik, L. Yusung, and H. Park, "Performance analysis of MIMO system with linear MMSE receiver," *IEEE Trans. on Wireless Commun.*, vol. 7, no. 11, pp. 4474–4478, Nov. 2008.

[50] H.V. Poor and S. Verdu, "Probability of error in MMSE multiuser detection," *IEEE Trans. Inform. Theory*, vol. 43, no. 3, pp. 858–871, May 1997.

[51] V. Tarokh, A. Naguib, N. Seshadri, and A.R. Calderbank, "Space-time codes for high data rate wireless communication: performance criteria in the presence of channel estimation errors, mobility, and multiple paths," *IEEE Trans. Commun.*, vol. 47, no. 2, pp. 199–207, Feb 1999.

[52] P. Soldati, M. Johansson, G. Fodor, and S. Sorrentino, "On pilot dimensioning in multicell single input multiple output systems," *in Proc. IEEE GLOBECOM Workshops*, pp. 1382–1387, Dec. 2011.

[53] T. Weber, A. Sklavos, and M. Meurer, "Imperfect channel-state information in MIMO transmission," *IEEE Trans. Commun.*, vol. 54, pp. 543–552, March 2006.

[54] M. Medard, "The effect upon channel capacity in wireless communications of perfect and imperfect knowledge of the channel," *IEEE Trans. Inform. Theory*, vol. 46, pp. 933–946, May 2000.

[55] L.L. Chong and L.B. Milstein, "The effects of channel estimation errors on a space-time spreading CDMA system with dual transmit and dual receive diversity," *IEEE Trans. Commun.*, vol. 52, pp. 1145–1151, July 2004.

[56] M.J. Gans, "The effect of gaussian error in maximal ratio combiners," *IEEE Trans. Commun. Tech.*, vol. 19, no. 4, pp. 490–500, Aug. 1971.

[57] B.R. Tomiuk, N.C. Beaulieu, and A.A. Abu-Dayya, "General forms for maximal ratio diversity with weighting errors," *IEEE Trans. Commun.*, vol. 47, no. 4, pp. 488–492, April 1999.

[58] B.R. Tomiuk, N.C. Beaulieu, and A.A. Abu-Dayya, "Maximal ratio combining with channel estimation errors," *in Proc. IEEE Pacific Rim Conf. Communications, Computers and Signal Processing*, pp. 363–366, May 1995.

[59] A. Annamalai and C. Tellambura, "Analysis of hybrid selection/maximal ratio diversity combiners with gaussian errors," *IEEE Trans. on Wireless Commun.*, vol. 1, no. 3, pp. 498–512, July 2002.

[60] W.M. Gifford, M.Z. Win, and M. Chiani, "Diversity with practical channel estimation," *IEEE Trans. on Wireless Commun.*, vol. 4, no. 4, pp. 1935–1947, July 2005.

[61] L. Chung Chu and U. Mitra, "Performance analysis of an improved MMSE multiuser receiver for mismatched delay channels," *IEEE Trans. Commun.*, vol. 46, no. 10, pp. 1369–1380, Oct. 1998.

[62] H. Li and H.V. Poor, "Impact of imperfect channel estimation on turbo multiuser detection in DS-CDMA systems," *in Proc. IEEE Wireless Commun. Network*, pp. 30–35, March 2004.

[63] B. Xia, J. Wang, and M. Sawahashi, "Performance comparison of optimum and MMSE receivers with imperfect channel estimation for VSF-OFCDM systems," *IEEE Trans. Wireless Commun.*, vol. 4, no. 6, pp. 3051–3062, Nov. 2005.

[64] M. Krondorf, T.J. Liang, and G. Fettweis, "Symbol error rate of OFDM systems with carrier frequency offset and channel estimation error in frequency selective fading channels," *in Proc. IEEE Intl. Conf. Commun.*, pp. 5132–5136, June 2007.

[65] Z. Zhang and C. Tellambura, "The effect of imperfect carrier frequency offset estimation on an OFDMA uplink," *IEEE Trans. Commun.*, vol. 57, pp. 1025–1030, April 2009.

[66] R. Narasimhan, "Performance of diversity schemes for OFDM systems with frequency offset, phase noise, and channel estimation errors," *IEEE Trans. Commun.*, vol. 50, no. 10, pp. 1561–1565, Oct. 2002.

[67] T. Peng and N.C. Beaulieu, "Precise BER analysis of p/4-DQPSK OFDM with carrier frequency offset over frequency selective fast fading channels," *IEEE Trans. on Wireless Commun.*, vol. 6, no. 10, pp. 3770–3780, Oct. 2007.

[68] Z. Zhang, W. Zhang, and C. Tellambura, "BER of MIMO-OFDM systems with carrier frequency offset and channel estimation errors," *in Proc. IEEE Intl. Conf. Commun.*, pp. 5473–5477, Aug. 2007.

[69] M. Krondorf and G. Fettweis, "Numerical performance evaluation for alamouti space time coded OFDM under receiver impairments," *IEEE Trans. on Wireless Commun.*, vol. 8, no. 3, pp. 1446–1455, March 2009.

[70] A.P. Liavas and D. Tsipouridou, "Single-carrier systems with MMSE linear equalizers: performance degradation due to channel and CFO estimation errors," *IEEE Trans. Signal Process.*, vol. PP, no. 99, 2012.

[71] V. Tarokh, A.F. Naguib, N. Seshadri, and A.R. Calderbank, "Space-time codes for high data rate wireless communication: mismatch analysis," *in Proc. IEEE Intl. Conf. Commun.*, vol. 1, pp. 309–313, June 1997.

[72] B. Morshed and B. Shahrrava, "A new metric for space-time block codes with imperfect channel estimates," *in Proc. IEEE WiMob, Montreal, Canada*, pp. 174–181, Aug. 2005.

[73] Y. Chen and N.C. Beaulieu, "Maximum likelihood receivers for space-time coded MIMO systems with gaussian estimation errors," *IEEE Trans. Commun.*, vol. 57, no. 6, pp. 1712 –1720, June 2009.

[74] H. Qinfei, M. Ghogho, and W. Jibo, "Data detection in cooperative STBC-OFDM systems with multiple frequency offsets," *IEEE Signal Process. Letters*, vol. 16, no. 7, pp. 600–603, July 2009.

[75] W. Hou, X. Wang, and G. Liu, "ML detection with successive group interference cancellation for interleaved OFDMA uplink," *IEEE Commun. Letters*, vol. 16, pp. 34–36, Jan. 2012.

[76] F. Gao, T. Cui, A. Nallanathan, and C. Tellambura, "Maximum likelihood detection for differential unitary space-time modulation with carrier frequency offset," *IEEE Trans. Commun.*, vol. 56, no. 11, pp. 1881–1891, Nov. 2008.

[77] S. Sun and Y. Jing, "Channel training design in amplify-and-forward MIMO relay networks," *IEEE Trans. Wireless Commun.*, vol. 10, no. 10, pp. 3380–3391, Oct. 2011.

Appendix A

Mathematical Calculations

This Appendix shows detail mathematical derivations and values which are used across the thesis. The novel algorithms proposed in Chater 4 uses various expression for different detection techniques. The values of these expressions are calculated in this Appendix. Section A.1 introduces the initial assumptions made for CFO and the conditional PDF of CAFO with its estimate is derived. In section A.2, the PDF given earlier is used for deriving the expected value of CAFO function conditioned on its estimate. These values are further used in calculating the expectation and variance of the received signal conditioned on imperfect estimates, in section A.3 and section A.4 respectively.

A.1 Conditional PDF of CAFO

CFO is a term used to represent the mismatch between the receiver oscillator frequency and carrier frequency of the transmitted signal which is given as

$$\triangle f = f_c - f_r$$

and the baseband signal at the k-th receive antenna with CFO is

$$r_k = \alpha_k s e^{j\phi_k} \sqrt{E_s} + n_k. \tag{A.1}$$

Here, ϕ_k is the CAFO with a sampling frequency f_s

$$\phi_k = \frac{2\pi \triangle f_k}{f_s}.$$

Let us assume, that the CAFO $\phi_k \sim \mathcal{N}\left(0, \sigma_\phi^2\right)$ is a zero mean Gaussian RV with variance σ_ϕ^2. It follows the distribution function given as

$$f_\phi\left(\phi_k\right) = \frac{1}{\sqrt{2\pi\sigma_\phi^2}} e^{\left(\frac{-{\phi_k}^2}{2\sigma_\phi^2}\right)}. \tag{A.2}$$

The estimator of CAFO, regardless of its type is modeled as

$$\hat{\phi_k} = \phi_k + \varepsilon_k,$$

where the estimation error $\varepsilon_k \sim \mathcal{N}\left(0, \sigma_\varepsilon^2\right)$ is taken as a zero mean Gaussian RV having variance σ_ε^2 and thus it is evident that the CAFO estimate $\hat{\phi}_k \sim \mathcal{N}\left(0, \sigma_{\hat{\phi}}^2\right)$ is also a zero mean Gaussian RV with variance $\sigma_{\hat{\phi}}^2$. The original value of CAFO ϕ_k and its estimate $\hat{\phi}_k$ are dependent on each other by the correlation coefficient

$$\begin{aligned}
\gamma &= \frac{E\left[\phi_k \hat{\phi}_k\right]}{\sqrt{\sigma_\phi^2 \sigma_{\hat{\phi}}^2}} \\
&= \frac{E\left[\phi_k\left(\phi_k + \varepsilon_k\right)\right]}{\sqrt{\sigma_\phi^2 \sigma_{\hat{\phi}}^2}} \\
&= \frac{\sigma_\phi^2}{\sqrt{\sigma_\phi^2 \sigma_{\hat{\phi}}^2}} \qquad \because \quad \phi_k \perp \varepsilon_k \\
&= \sqrt{1 - \frac{\sigma_\varepsilon^2}{\sigma_{\hat{\phi}}^2}}.
\end{aligned}$$

Using the relations for bi-variate Gaussian distributions given in standard literature, we get the expected value ϕ_k conditioned on $\hat{\phi}_k$ as

$$\begin{aligned}
E\left[\phi_k | \hat{\phi}_k\right] &= \frac{\gamma \sigma_{\phi_k} \hat{\phi}_k}{\sigma_{\hat{\phi}_k}} \\
&= \gamma^2 \hat{\phi}_k
\end{aligned} \tag{A.3}$$

and the conditional variance as

$$\begin{aligned} Var\left[\phi_k|\hat{\phi}_k\right] &= \left(1-\gamma^2\right)\sigma_{\phi_k}^2 \\ &= \sigma_\varepsilon^2\gamma^2. \end{aligned} \tag{A.4}$$

With the above relations, it is easily shown that the conditional PDF of ϕ_k given $\hat{\phi}_k$ is

$$f_{\phi|\hat{\phi}}\left(\phi_k|\hat{\phi}_k\right) = \frac{1}{\sqrt{2\pi\sigma_\varepsilon^2\gamma^2}} e^{\frac{-\left|\phi_k-\gamma^2\hat{\phi}_k\right|^2}{2\sigma_\varepsilon^2\gamma^2}}. \tag{A.5}$$

The above PDF will be used in the next chapter for further derivation.

A.2 Conditional Expectation of CAFO

In this section, the conditional expectation of the function of CAFO with the estimate is calculated. From the expression of baseband signal given in (A.1) and the PDF derived in (A.5), we can calculate

$$\begin{aligned} E\left[e^{j\phi_k}\middle|\,\hat{\phi}_k\right] &= \int_{-\infty}^{\infty} e^{j\phi_k} f_{\phi|\hat{\phi}}\left(\phi_k|\hat{\phi}_k\right) d\phi \\ &= \int_{-\infty}^{\infty} \frac{e^{j\phi_k}}{\sqrt{2\pi\sigma_\varepsilon^2\gamma^2}} e^{\frac{-\left|\phi_k-\gamma^2\hat{\phi}_k\right|^2}{2\sigma_\varepsilon^2\gamma^2}} d\phi \end{aligned} \tag{A.6}$$

Let $a = 2\sigma_\varepsilon^2\gamma^2$ and $b = \gamma^2\hat{\phi}_k$, thus the above equation becomes

$$E\left[e^{j\phi_k}\middle|\,\hat{\phi}_k\right] = \frac{1}{\sqrt{a\pi}} \int_{-\infty}^{\infty} e^{j\phi_k} e^{\frac{-|\phi_k-b|^2}{a}} d\phi. \tag{A.7}$$

Again, let $z = \phi_k - b \Rightarrow dz = d\phi$ and $\phi_k = z + b$.

$$\begin{aligned} E\left[e^{j\phi_k}\middle|\,\hat{\phi}_k\right] &= \frac{1}{\sqrt{a\pi}}\int_{-\infty}^{\infty} e^{j(z+b)}e^{\left(-z^2/a\right)}dz \\ &= \frac{e^{jb}}{\sqrt{a\pi}}\int_{-\infty}^{\infty} e^{jz}e^{\left(-z^2/a\right)}dz \\ &= e^{jb}e^{(-a/4)}. \end{aligned} \tag{A.8}$$

Substituting the values of a and b

$$E\left[e^{j\phi_k}\middle|\,\hat{\phi}_k\right] = e^{\left(-0.5\sigma_{\tilde{\varepsilon}}^2\gamma^2 + j\gamma^2\hat{\phi}_k\right)}. \tag{A.9}$$

A.3 Conditional Expectation of Received Signal

According to the assumptions made earlier in the thesis, the channel fading parameter $\alpha_k \sim \mathcal{N}(0,1)$ is a zero mean Gaussian RV with unit variance. The imperfect channel estimate $\hat{\alpha}_k \sim \mathcal{N}(0,\sigma_{\hat{\alpha}}^2)$, its estimation error $\epsilon_k \sim \mathcal{N}(0,\sigma_{\epsilon}^2)$ and the AWGN $n_k \sim \mathcal{N}(0,N_0)$ also follow Gaussian distribution with mean zero with variances $\sigma_{\hat{\alpha}}^2$, σ_{ϵ}^2 and N_0 respectively. The correlation coefficient between α_k and $\hat{\alpha}_k$ is given as

$$\rho = \frac{1}{\sqrt{1+\sigma_{\epsilon}^2}}.$$

Here, the results given in [51] are directly used, which are as follows

$$\begin{aligned} E\left[\alpha_k|\hat{\alpha}_k\right] &= \frac{\rho\hat{\alpha}_k}{\sigma_{\hat{\alpha}}} \\ Var\left[\alpha_k|\hat{\alpha}_k\right] &= 1-\rho^2 \\ E\left[r_k|\hat{\alpha}_k\right] &= \frac{\rho\hat{\alpha}_k\sqrt{E_s}s}{\sigma_{\hat{\alpha}}} \\ Var\left[r_k|\hat{\alpha}_k\right] &= N_0 + \left(1-\rho^2\right)E_s\left|s\right|^2. \end{aligned} \tag{A.10}$$

Now, let us calculate the expected value of the received signal r_k conditioned on the channel estimate $\hat{\alpha}_k$ and the CFO estimate $\hat{\phi}_k$. Thus from (A.1) and (A.9),

$$\begin{aligned} E\left[r_k \left| \hat{\alpha}_k, \hat{\phi}_k \right.\right] &= E\left[\alpha_k | \hat{\alpha}_k\right] \sqrt{E_s} s E\left[e^{j\phi_k} \left| \hat{\phi}_k \right.\right] \\ &= \frac{\rho \hat{\alpha}_k}{\sigma_{\hat{\alpha}}} \sqrt{E_s} s e^{\left(-0.5\sigma_{\tilde{\varepsilon}}^2 \gamma^2 + j\gamma^2 \hat{\phi}_k\right)}. \end{aligned} \tag{A.11}$$

Let us consider the parameter introduced in (4.20)

$$z_k = \alpha_k e^{j\phi_k}.$$

We can calculate the expectation of z_k conditioned on $\hat{\alpha}_k$ and $\hat{\phi}_k$ as

$$\begin{aligned} E\left[z_k \left| \hat{\alpha}_k, \hat{\phi}_k \right.\right] &= E\left[\alpha_k | \hat{\alpha}_k\right] E\left[e^{j\phi_k} \left| \hat{\phi}_k \right.\right] \\ &= \frac{\rho \hat{\alpha}_k}{\sigma_{\hat{\alpha}}} e^{\left(-0.5\sigma_{\tilde{\varepsilon}}^2 \gamma^2 + j\gamma^2 \hat{\phi}_k\right)}. \end{aligned} \tag{A.12}$$

A.4 Conditional Variance of Received Signal

In the section, the aim is to calculate the variance of received signal r_k conditioned on the channel estimate $\hat{\alpha}_k$ and the CFO estimate $\hat{\phi}_k$. To obtain this, we need to do some preliminary calculations. Using (A.10), it can be easily written

$$\begin{aligned} E\left[\left|\alpha_k\right|^2 \left| \hat{\alpha}_k \right.\right] &= Var\left[\alpha_k \left| \hat{\alpha}_k \right.\right] + \left(E\left[\alpha_k \left| \hat{\alpha}_k \right.\right]\right)^2 \\ &= 1 - \rho^2 + \frac{\rho^2 \left|\hat{\alpha}_k\right|^2}{\sigma_{\hat{\alpha}}^2}. \end{aligned} \tag{A.13}$$

We can easily say from the relation of z_k,

$$E\left[\left|z_k\right|^2 \left| \hat{\alpha}_k, \hat{\phi}_k \right.\right] = E\left[\left|\alpha_k\right|^2 \left| \hat{\alpha}_k \right.\right].$$

Now, we calculate the second moment of the received signal r_k conditioned on $\hat{\alpha}_k$ and $\hat{\phi}_k$

$$\begin{aligned} E\left[\left|r_k\right|^2 \left| \hat{\alpha}_k, \hat{\phi}_k \right.\right] &= E\left[\left|\alpha_k\right|^2 \left| \hat{\alpha}_k \right.\right] E_s \left|s\right|^2 + \sigma_n^2 \\ &= \left(1 - \rho^2 + \frac{\rho^2 \left|\hat{\alpha}_k\right|^2}{\sigma_{\hat{\alpha}}^2}\right) E_s \left|s\right|^2 + N_0. \end{aligned} \tag{A.14}$$

Using the above result and from (A.11), we can easily calculate the variance of r_k conditioned on $\hat{\alpha}_k$ and $\hat{\phi}_k$

$$\begin{aligned} Var\left[|r_k|^2 \left| \hat{\alpha}_k, \hat{\phi}_k \right.\right] &= E\left[|r_k|^2 \left| \hat{\alpha}_k, \hat{\phi}_k \right.\right] - \left(E\left[r_k \left| \hat{\alpha}_k, \hat{\phi}_k \right.\right]\right)^2 \\ &= N_0 + E_s|s|^2(1-\rho^2) + \left(1 - e^{\left(-\sigma_{\tilde{\varepsilon}}^2 \gamma^2\right)}\right) \frac{\rho^2 E_s |s|^2 \hat{\alpha}_k^2}{2\sigma_{\hat{\alpha}}^2}. \end{aligned} \tag{A.15}$$

Vita Auctoris

NAME	:	Shayondip Sinha
BIRTH YEAR	:	1984
BIRTH PLACE	:	INDIA
EDUCATION		
2010–2012	:	**Masters of Applied Science**
		Electrical and Computer Engineering
		University of Windsor, Windsor, Ontario, Canada
2003–2007	:	**Bachelors of Engineering**
		Electronics and Electrical Engineering
		Sathyabama University, Chennai, India